Journal of Sound and Vibration (2001) **239**(4), 731–765
doi:10.1006/jsvi.2000.3226, available online at http://www.idealibrary.com on IDEAL®

SOUND TRANSMISSION THROUGH DUCT WALLS

A. CUMMINGS

School of Engineering, University of Hull, Hull, East Yorkshire HU6 7RX, England.
E-mail: a.cummings@eng.hull.ac.uk

(*Accepted* 10 *July* 2000)

Acoustic "breakout" and "breakin" through duct walls had, until the late 1970s, been a rather neglected topic of research, particularly in the field of heating, ventilating and air-conditioning ducts. Since then, interest has grown and many publications have appeared in which predictive methods have been reported. Research in this area, especially that which has been conducted over the past two decades, is reviewed in this paper. Efforts are made to identify the main physical processes involved and to present some relevant published data, rather than to give a finely detailed, comprehensive, account of this research. Some comments are made concerning the possible direction of future research.

1. INTRODUCTION

Acoustic "breakout" and "breakin" through duct walls is an important problem in engineering acoustics. One of the commonest applications is in heating, ventilating and air-conditioning (HVAC) and other gas flow ducting (such as large industrial silencers), where the duct walls may be made from fairly thin sheet metal. Internal noise transmitted through the walls of ventilating ducts into offices or other building spaces can be a problem [1, 2], particularly at low frequencies. Flanking transmission in lined ducts and silencers can be caused in part by breakout and subsequent breakin (in which case it may be termed "radiation bypass" transmission [3]). A (possibly) beneficial effect, caused by breakout, is "natural" duct attenuation in unlined ducts [4], which is a consequence of noise breakout and involves a diminution of the internally propagated sound power. Provided the breakout does not occur in a noise-sensitive area, natural duct attenuation can be a useful way of reducing sound power levels in long runs of duct. In sheet metal ducts with flat walls, breakout and breakin effects are usually most important at low- to mid-frequencies.

Acoustic radiation from gas flow piping—for example, downstream from pressure control valves—is another case of interest. Here, the wall thickness would normally be greater than that of typical sheet metal and the pipe cross-section would be closely circular, with little of the distortion often encountered in circular sheet metal ducts. High-frequency noise would usually dominate the radiated spectrum, associated with higher order mode propagation effects inside the duct coupling to circumferential structural modes in the pipe wall [5]. Vehicle silencer "shell noise" is a further effect associated with noise breakout from elastic-walled ducts. It is a form of flanking transmission that bypasses the noise directly radiated from the silencer outlet.

Although there are many similarities in the physical processes involved, between acoustic breakout/breakin in ducts and sound transmission through building partitions, the differences in detail between these two phenomena have led to rather different approaches in modelling being adopted by most workers. In the case of building partitions, modelling is

0022-460X/01/040731 + 35 $35.00/0

usually based either on forced-wave transmission in an infinite panel or a modal response in the structure, with appropriate modal radiation efficiencies; statistical energy analysis (SEA) models include both resonant and non-resonant response of the partition. The acoustics of the spaces on either side of the partition may or may not be included in the model. Most of the models for duct wall breakout take the sound field inside the duct to be composed of one or more propagating modes [6] (either rigid duct modes or coupled structural/acoustic modes), in contrast to the more or less diffuse, reverberant sound field that is frequently assumed to exist within a building space. Sound radiation from a duct wall has been modelled in three ways: analytically as a finite-length line source [7–9], as a finite-length cylindrical (or equivalent cylindrical) radiator [9] or numerically by using finite element (FE) analysis [9, 10]; all three types of model have been based on axially travelling wave motion. These models contrast with those popular in the case of flat rectangular partitions, which often involve concepts and terminology drawn from modal phase cell patterns and phase cancellation effects, combined with relative structural and acoustic wavenumbers ("corner modes", "edge modes", "surface modes"; "acoustically fast", "acoustically slow" modes). In the case of sound radiation from ducts, it has usually been sufficient to consider forced-wave excitation of the duct walls by waves travelling in one direction only. Axially resonant structural or acoustic effects do not normally play a major role in duct wall breakout, though both acoustic and structural resonant effects in the cross-sectional plane of the duct are very important. The concept of coupled structural/acoustic duct modes is useful. It can be shown that these modes generally fall into the categories of "acoustic" (where most of the power flow in the mode is in the fluid) or "structural" (where most of the power flow is in the structure) [11, 12]. Such coupled modes may be used in summations to represent the total fluid/structural field [13, 14].

Aircraft fuselage structures appear at first to have some features in common with duct walls because of the tubular shape of aircraft but, here, the much more complex nature of aircraft structures and the different length scales and frequency ranges involved render different modelling techniques more appropriate. Often, the double-septum arrangement of outer skin and interior trim, bounded by stringers and frame stiffeners, is treated as an isolated panel or a small group of panels because of the immense complexity involved in analyzing the entire structure. The methods of analysis generally bear more resemblance to those of building partitions than those employed in ducts.

What may be the earliest attempt to predict duct wall breakout and breakin, briefly described by Allen [15], is based on the principles employed in building acoustics and is not valid in the low-frequency region where these effects are most pronounced. In the case of breakout, there are several reasons for this. In part, the difference between the implicitly assumed and actual radiation efficiency of the duct walls is responsible, and so is the assumed diffuseness of the incident sound field. The predictions are considerably at variance with measured data, particularly in terms of the frequency dependence of the wall transmission loss TL (defined in some appropriate way). Similar deficiencies are apparent in the case of the breakin formula given in reference [15]. Allen's breakout formula is, however, not greatly in error at high frequencies, at least for rectangular-section ducts. Webb [1] and Sharland [2] also give accounts of breakout. Sharland cites Allen's formula, but rightly points out that it will overestimate the sound power radiated from the walls of circular ducts at low frequencies.

The cross-sectional geometry of a duct has a great effect on breakout and breakin characteristics. The three most common cross-sectional shapes of air-moving ductwork are shown in Figure 1. They are rectangular, "flat-oval" (having two opposite flat walls and two opposite semicircular curved walls but fabricated from a single duct, originally of circular cross-section) and circular. Ideally circular section ducts have a very high TL at low

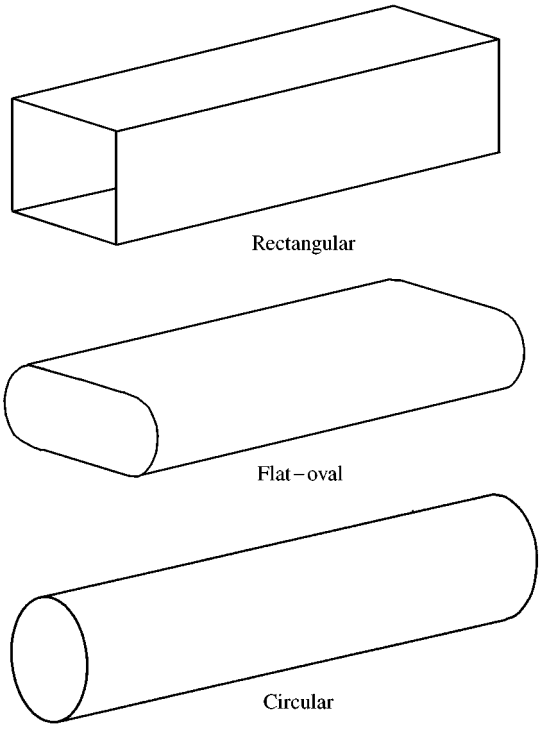

Figure 1. Cross-sectional shapes of air-moving ducts.

frequencies, and this at first falls monotonically as the frequency increases, so long as only the plane internal acoustic mode can propagate. Higher order internal mode propagation, coupled with higher structural mode excitation and/or the ring resonance of the duct wall, complicate the form of the TL curve, as does the wave coincidence effect. However, there is usually a negligible breakout or breakin problem in practice with circular ducts, so long as they are closely circular in cross-section. Distortion from circularity can bring about a "mode coupling" effect, whereby the plane internal acoustic mode excites higher structural modes in a distorted circular duct, considerably enhancing the radiated sound power and lowering the TL. Several authors (see, for example, references [10, 16–19]) have noted this. Closely circular ducts can have a lower wall TL than would be expected on the basis of plane mode theory if the lowest internal acoustic cross-mode is strongly excited at some point in the duct, even though it might not propagate. Whole-duct bending modes are excited, and radiate significant sound power, as was shown by Kuhn and Morfey [20]. Rectangular cross-section ducts tend to have the lowest breakout wall TL of all at low frequencies, because the structural response to the internal sound field is strong. Cummings [21, 22] and Guthrie [23] have investigated this. Ducts of flat–oval cross-section might, from a simple viewpoint, be expected to display the TL characteristics of both rectangular and circular ducts. Perhaps surprisingly (since a simple point of view rarely paints the whole picture), this is the case. Flat–oval ducts have the low-frequency TL characteristics of rectangular ducts, and also display a ring resonance like that of circular ducts at the expected frequency for a circular duct of the same diameter as the circularly curved sides. Cummings and Chang [24, 25] compare both simplified analytical and numerical TL models to measured data, and also describe models for sound propagation in rigid flat–oval waveguides [26].

Various analytical and numerical methods have been employed in the modelling of duct wall breakout and breakin. Cummings *et al.* [6, 8, 10, 11, 21, 22, 24, 27] have employed a number of approximate analytical methods in modelling rectangular, distorted circular and flat–oval ducts. The simplifications made in the models include quasi-one-dimensional approximations for sound fields in ducts, the neglect of structural/acoustic coupling between the wall motion and internal and/or external sound fields, and (as mentioned earlier) the idealization of complicated radiating surfaces by simpler shapes such as circular cylinders and line sources. Relatively simple one-dimensional coupled structural/acoustic mode models have been employed by Cummings [4, 11, 21, 22], who also used an uncoupled forced-wave approach [6, 24, 27] to treat higher order acoustic mode transmission in ducts with elastic walls. Fourier series formulations have been used by Cummings *et al.* [10] and Cabelli [12]. Time-independent finite difference (FD) methods were used by Chang and Cummings [19, 25] and a time-dependent FD method was employed by Cabelli [28]. A Rayleigh–Ritz treatment was used by Cummings and Astley [14] and FE methods have been employed by Astley *et al.* [9, 13], Martin [29] and Kirby and Cummings [30, 31].

The implementation of any accurate predictive model for duct wall breakout and breakin requires considerable programming effort and is not normally possible within the scope of typical engineering design projects involving noise control on gas flow ducting. In an effort to bridge the gap between theory and practicality, the author has published design charts [32] for breakout of TL prediction, which involve the use of dimensionless parameters and can be used with minimal effort to yield quite accurate TL plots for a wide range of duct parameters. He also contributed toward the 1984 ASHRAE Systems Handbook [33] in the form of simple predictive schemes for noise breakout from rectangular and flat–oval section ducts. Included amongst these practical tools is a method for predicting the insertion loss of external wall lagging (see also reference [34]), which is sometimes applied in an attempt to reduce noise breakout. A further possible method of breakout noise reduction in rectangular ducts is to stiffen the duct walls so as to raise the fundamental transverse structural resonance frequency of the walls so that it is above the frequency region where problems are likely to exist. This idea seems not to have taken root amongst duct designers, even though Cummings [11] showed that substantial improvements in the breakout TL could be achieved by the use of laminated composite wall structures designed to have a high stiffness/mass ratio. So-called "cross-breaking"—the introduction of diagonal creases in duct wall panels so as to form a very shallow outward-pointing pyramid—is sometimes applied to the walls of rectangular ducts in an effort to increase their rigidity and promote resistance to buckling as the internal pressure changes. There was—and perhaps still is—a belief amongst HVAC engineers that cross-breaking must increase the breakout TL of the duct walls significantly. This has, however, been shown experimentally [35] not to be the case.

The effects of sound-absorbing linings on duct wall breakout and breakin were implicit in the study by Astley *et al.* [13], although the emphasis in this work was on the effects of wall flexibility on sound propagation within the duct, rather than radiation to the exterior by the walls. Cummings and Astley [14], in their investigation of flanking mechanisms in lined ducts, modelled wall flexibility effects on breakout and breakin. These effects have been included in recent studies by Kirby and Cummings [31], who also modelled for the first time the effects of mean gas flow in the duct [30, 31]. Gas flow effects on the breakout TL were shown [31] to be quite small at typical mean flow Mach numbers, and this may be taken as justification for the neglect of flow in previous research.

Perhaps the main physical phenomena that have not been investigated in any detail in previous work are those resulting from acoustic and structural reflections at axial

discontinuities such as abrupt area changes, duct lining terminations, structural joints and flanges, and transitions between duct wall-sections of differing thickness. Results published by Astley *et al.* [13] indicate that the transition between rigid and flexible walls in a duct of uniform cross-section gives rise to a series of coupled structural/acoustic modes when the plane acoustic mode is incident from the rigid section. This is to be expected on the basis that a combination of modes would be required in order to satisfy all structural and acoustic boundary conditions.

An excellent review of research on duct wall breakout prior to 1982 was given by Almgren [36], but almost two decades have passed since its publication and much research has been conducted within this period. The purpose of the present paper is to summarize research on duct wall breakout and breakin to the present, and to highlight the important physical effects governing these phenomena.

2. PHYSICAL PHENOMENA

In this section, a summary of the important physical phenomena governing acoustic breakout and breakin is given.

2.1. COUPLED MODES

One of the principal physical effects exhibited in acoustic propagation in elastic-walled ducts is the coupling between fluid and structure. Coupled wave solutions to the governing acoustic and structural wave equations are those in which the fluid and structural waves have identical wavenumbers, whether these are real, imaginary or complex. Fahy [37] gives an excellent account of two-dimensional structural/acoustic wave coupling in a system consisting of a fluid layer sandwiched between two identical *infinite* thin flexible plates that undergo purely bending motion. He first derives the dispersion equation, and then considers various special cases as a way of providing a clear physical interpretation of the wave coupling phenomena. Typical dispersion plots are also given. Fahy describes the rather complicated behaviour of both evanescent and propagating coupled mode solutions to the dispersion equation and highlights various features of the problem such as the role of the mass–air–mass resonance, the critical frequency of coincidence and the limiting cases of infinitely massive and completely massless walls.

In the case of ducts, the walls are of finite extent around the duct perimeter, and therefore additional effects, associated with transverse structural wave motion, occur. Broadly, these add what are essentially free structural wave "cut-on" effects (which have no parallel in the situation considered by Fahy) to the other structural/acoustic coupled wave phenomena. Cummings [21] noted transverse wall resonance effects in an early investigation of acoustic breakout at low frequencies through the walls of rectangular ducts. Later [11], he recognized the role of structural wave cut-on in "structural"-type coupled modes (with a plane-wave approximation for the internal sound field), in which most of the total power flow occurs in the duct walls (as distinct from "acoustic"-type modes in which the fluid carries most of the power flow). These modes behave much like free structural waves, except close to their cut-on frequencies, but even so these frequencies are close to those for free structural waves. An important feature of structural-type coupled modes is that the sound pressure within the duct is relatively very small—becoming smaller, the closer the modal phase speed is to the free structural wave speed—as compared to the structural amplitude (both amplitudes being expressed in an appropriate dimensionless form). For a thin plate of

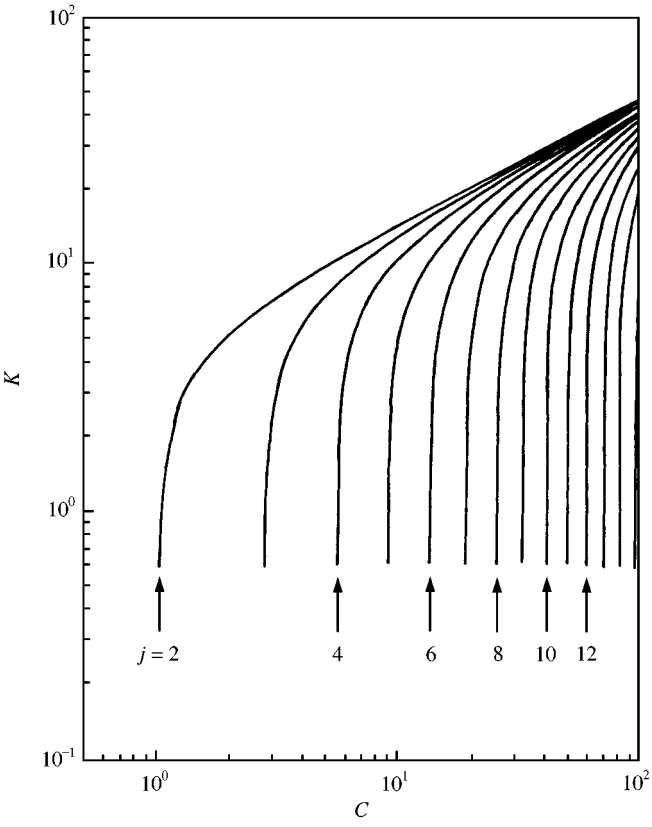

Figure 2. Roots of the dispersion equation for free structural waves *in vacuo*, in a strip of thin plate with clamped edges [11]. The number of nodes in the transverse displacement pattern is denoted by *j*.

uniform width a, clamped along both edges, the dispersion equation for free travelling structural modes *in vacuo* is [11]

$$(5{\cdot}144C^2\pi^4 - K^4)^{1/2}\{1 - \cos[(2{\cdot}268C\pi^2 - K^2)^{1/2}]\cosh[(2{\cdot}268C\pi^2 + K^2)^{1/2}]\}$$

$$+ K^2 \sin[(2{\cdot}268C\pi^2 - K^2)^{1/2}]\sinh[(2{\cdot}268C\pi^2 + K^2)^{1/2}] = 0, \quad (1)$$

where $C = f/f_{(2)}$, f is the frequency, $K = k_x a$, k_x is the modal wavenumber in the direction of propagation and $f_{(2)}$ is the fundamental resonance frequency of a beam with clamped ends, consisting of a transverse slice of the plate. Roots of equation (1) are shown in Figure 2 and illustrate how k_x, in dimensionless form, depends on the dimensionless frequency. This plot is also valid for symmetrical free structural waves in a square-section duct, where all four corners exhibit neither translational nor rotational motion. The infinity of roots of this transcendental equation suggests the existence of a correspondingly infinite number of coupled "structural"-type modes. This is the case, though in reality the coupled modes become more complex in nature as the internal sound field deviates significantly from plane. However, the similarity to free structural waves persists.

Astley [38] outlined a Rayleigh–Ritz formulation from which coupled mode parameters in an acoustically lined duct with flat flexible walls may be found, and applied it to a lined

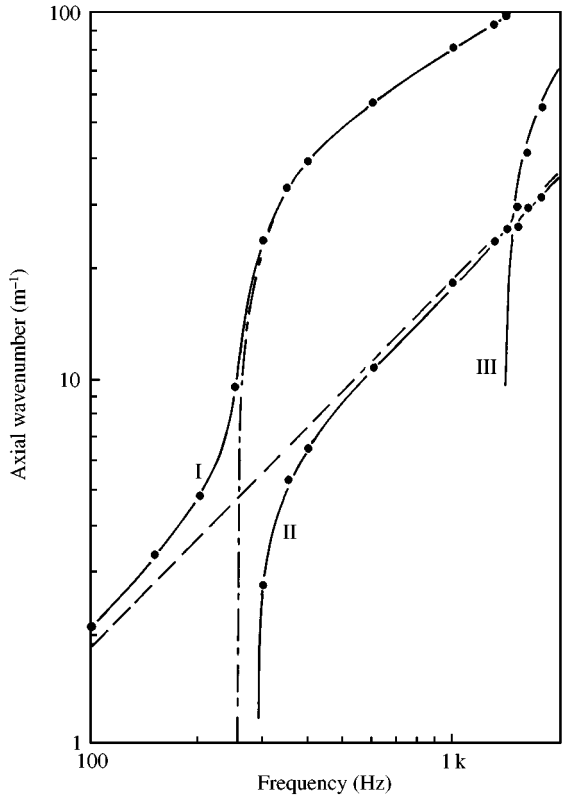

Figure 3. Predictions of the axial wavenumber for three coupled modes in a duct with three rigid walls and one flexible wall [13] (transverse duct dimensions 90 mm × 100 mm; one of the 100 mm walls is of 0·54 mm aluminium plate). ———, plane-wave approximation; ●, FE solution; — — —, plane wave in rigid-walled duct; — – —, free structural mode corresponding to coupled mode I.

rectangular duct with one flexible wall, via a uniform sound pressure approximation for the internal sound field. Comparison is made, in this paper, with both measured data and an FE formulation. The Rayleigh–Ritz method works surprisingly well, though it breaks down in the region of cut-on for the first structural-type coupled mode, the reason for this being that if fails to model adequately the non-uniform sound field in the lined duct, in this frequency region. Astley *et al.* [13] present detailed comparisons between FE predictions, measured data and a plane-wave approximation for the same experimental duct as that studied in reference [38], both with and without a lining. The duct measured 90 mm × 100 mm and had one flexible wall, of aluminium 0·54 mm thick, as one of its longer sides. It is shown in reference [13] that the plane-wave approximation works well in predictions of coupled mode wavenumbers for the unlined duct and, indeed, the numerical data are almost indistinguishable from the FE predictions. The roles of the coupled modes are discussed. Some of these predictions are shown in Figure 3. The dashed line here represents the wavenumber of the plane rigid-wall duct mode, $k_x = \omega/c$, where ω is radian frequency and c is the sound speed. The solid lines, representing the plane mode approximate solution, and the circle symbols, denoting the FE predictions, almost coincide. Mode I has, at low frequencies, a subsonic wave speed consistent with a spring-like wall impedance. It has most of its power flow in the air inside the duct. The cut-on frequency for the first free structural

mode is 260 Hz, and close to this frequency, mode I undergoes a transition to free structural mode behaviour. Above 260 Hz, this mode carries most of its power flow in the structure. Meanwhile, a new mode, mode II appears, initially resembling an acoustic-type mode, with a highly supersonic phase speed (corresponding to a mass-like wall impedance) just above structural mode cut-on at 260 Hz, which approaches the acoustic speed as the frequency rises. It is, in this region, an "acoustic"-type mode. At about 1·5 kHz, the cut-on frequency for the second free structural mode, mode II undergoes a transition to a structural-type mode in much the same way as mode I does at the lower cut-on frequency. A new mode—mode III appears—and this pattern is repeated as the frequency rises. Acoustic higher order mode cut-on effects complicate this general behaviour, however, at higher frequencies. At any given frequency, there is *only one* acoustic-type mode, except in the vicinity of transverse wall resonances, though there may be one or more structural-type modes.

Cabelli [12], using a Fourier series representation of the sound field in the duct, presents axial wavenumber predictions for coupled modes and predictions of the relative sound power in structural and acoustic mode types, for a square duct with one elastic wall. He includes coupled mode types that are the equivalents of higher order modes in a rigid-walled duct. Comparisons between Cabelli's predicted coupled modal axial wavenumber data (for a non-uniform internal sound field) and those based on a plane-mode approximation show very close agreement between the two up to the cut-on frequency of the first acoustic higher order mode in the equivalent rigid-walled duct, as in reference [13]. The quasi-plane-mode formulation of Cummings [21] is adequate for comparison purposes. In this, a dispersion equation is written

$$k_x/k - \sqrt{1 - \mathrm{i}L\langle\beta\rangle/kS} = 0, \tag{2}$$

where $k = \omega/c$, L is the perimeter of the duct, S is its cross-sectional area and $\langle\beta\rangle$ is the average of the dimensionless wall admittance around the perimeter. In the case of a rectangular duct, the wall admittance is found from solutions to the thin-plate equation, subject to boundary conditions at the duct corners, where the normal wall displacement is put equal to zero, the bending moments about the corners are equated in adjacent walls and the corners are assumed to remain right-angled. This procedure requires the solution of a system of eight linear equations.

The general behaviour of coupled modes noted by Astley *et al.* [13] and Cabelli [12] in the case of a duct with one flexible wall also applies to rectangular ducts with four elastic walls [14, 30, 31], both with and without sound-absorbing linings. In the case of lined ducts, the structural type modes can constitute a *direct* structural flanking path (in contrast to the indirect radiation bypass mechanism [3]), in which structure-borne energy flow bypasses the duct lining and can re-radiate into the fluid in the duct where there is a discontinuity such as a joint, or perhaps a silencer termination. On the other hand, structural resonance in a duct wall can enormously enhance the attenuation in a silencer. Astley *et al.* [13] have demonstrated this effect in a case where the duct lining is placed against a flexible wall, and their results are reproduced in Figure 4. In a narrow band around the lowest wall resonance frequency, the attenuation (in dB/m) is dramatically increased to a value about 10 times that in the equivalent rigid-walled duct. There is a broader frequency band, about one octave wide, over which the attenuation is significantly increased by this wall resonance effect. The mechanism is a kind of "gas-pumping" process in which the air adjacent to the flexible wall is forced through the pores of the absorbent at an enhanced particle velocity. The wall panel and lining together act as a damped resonant absorber.

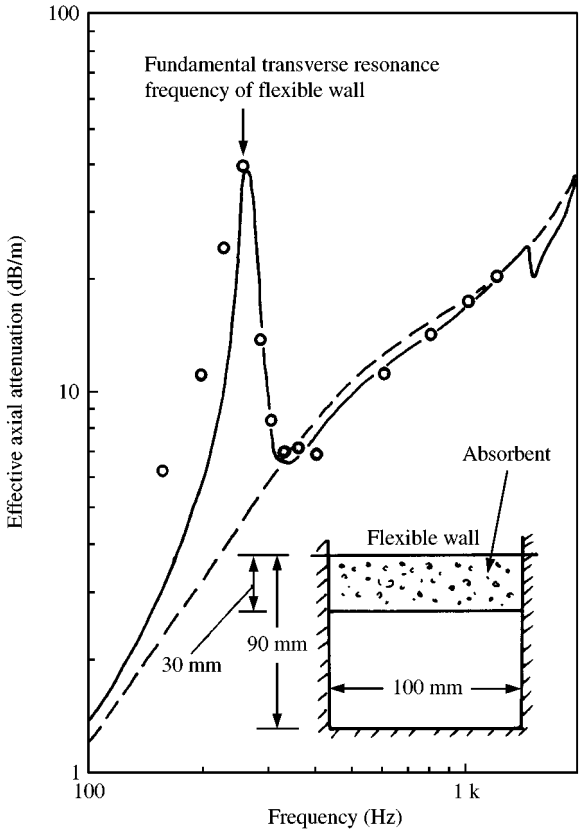

Figure 4. Effective axial attenuation per unit length in a duct with three rigid walls and one flexible wall, containing an acoustic lining [13] (polyurethane foam, steady flow resistivity 6230 mks rayl/m; flexible wall, 0·54 mm aluminium). ———, FE solution; ○, measured; — — —, rigid-walled duct.

2.2. THE EFFECTS OF DUCT CROSS-SECTIONAL GEOMETRY

Here, four cross-sectional shapes are considered: rectangular, flat-oval, circular and distorted circular. Between them, these cover almost all the duct geometries in common use. We will discuss the breakout TL here, as a parameter representative of both breakout and—as will be seen in section 2.4—breakin. Various definitions of the breakout TL have been given in the literature, but the following is the most popular:

$$TL = 10 \log\left(\frac{W_i/A_i}{W_r/A_r}\right), \tag{3}$$

where W_i and W_r are, respectively, the sound power entering the duct and radiated by the duct walls, and A_i, A_r are, respectively, the duct cross-sectional area and the radiating area.

2.2.1. *Rectangular cross-section*

In the case of rectangular ducts, the breakout TL typically exhibits an overall positive slope of 3 dB/octave at low- to mid-frequencies [6]. This tends to increase to about 6 dB/octave at higher frequencies, where many acoustic modes can propagate in the duct. This basic form of the TL curve results from mass control of the wall impedance, but

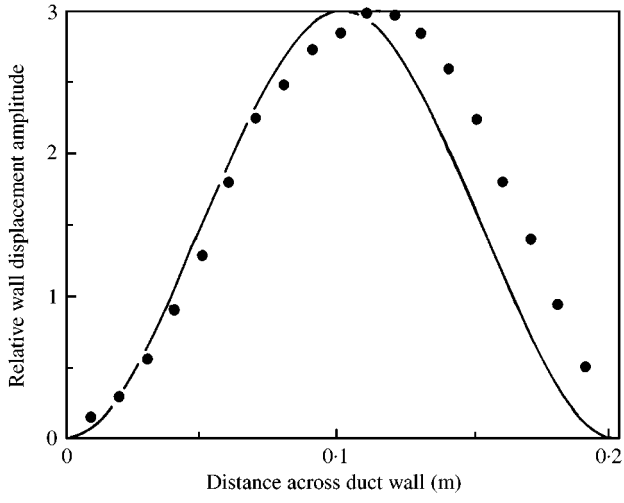

Figure 5. Measured, ●, predicted, ———, vibration displacement amplitude profile on one wall of a square section mild steel duct [21] (203 mm square, wall thickness 1·22 mm). Frequency = 277 Hz.

superimposed on it are undulations [6, 9, 21], which are caused by damped transverse structural resonances in the walls. The 3 dB/octave slope contrasts with the 6 dB/octave slope that is characteristic of sound transmission through a limp-mass, infinite partition. This may be explained on the basis of a finite length line source model for radiation from the duct walls (see section 2.3 and references [7, 8, 21, 27]). In this, an additional factor of ω appears, in the expression for radiated sound power, as compared to the case of the partition, which reduces the slope of the TL curve by 3 dB/octave. In Figure 5, is shown a comparison between measured and predicted relative wall displacement patterns on one wall of a 203 mm square section steel duct with 1·22 mm walls, excited by the plane internal acoustic mode [21]. These compare quite well, given that the experimental duct was not ideally constructed. It can be seen that—as one would expect—the wall displacement tends to fall to zero at the duct corners and reaches a maximum at the centre of the wall. Other comparisons between prediction and measurement [9, 21] on rectangular ducts with both the plane mode and a higher order internal mode are favourable and show that the assumed boundary conditions at the duct corners are realistic.

Measured TL data on a typical air-moving duct (galvanized steel, 457 mm × 229 mm, with 0·64 mm walls) are shown in Figure 6, and are compared to predictions based on the "wave solution" [21, 22] and "asymptotic mass law" [6] treatments of Cummings. In the latter approach, coupling between the internal sound field and the duct wall motion is ignored. It can be seen that the wave solution prediction is in good agreement with measured data. The asymptotic solution is also in good agreement, and exhibits a slope of 3 dB/octave except at low frequencies, where the relative transparency of the duct walls to sound brings about a more rapid fall of TL as the frequency drops. A prediction from the TL formula of Allen [15] is also plotted. This is

$$TL \approx 10 \log\left(\frac{m^2\omega^2}{12{\cdot}7\,\rho^2 c^2}\right) \tag{4}$$

for $(\omega m/2\rho c)^2 \gg 1$, where m is the mass per unit area of the duct wall and ρ is the air density. It can be seen that this is considerably at variance with the measured data, and has a slope of 6 dB/octave.

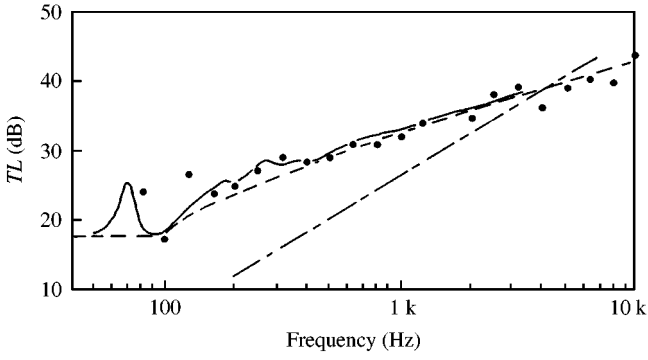

Figure 6. Fundamental mode transmission loss of a rectangular galvanized steel duct (457 mm × 229 mm cross-section, wall thickness 0·64 mm). ●, measurements [6]; ———, wave solution [21, 22]; — — —, asymptotic mass law [6], — – —, Allen's formula [15].

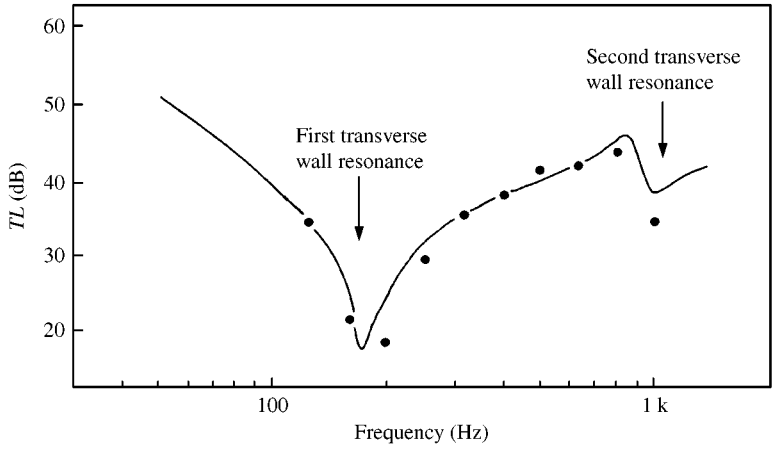

Figure 7. Fundamental mode transmission loss of 203 mm square section, 1·22 mm wall thickness, mild steel duct [21, 22]: ●, measured, ———, predicted.

An extreme case of wall resonance effects is shown in Figure 7. This duct was of fairly small, square, cross-section, with relatively thick walls (it is actually the duct whose wall displacement profile is shown in Figure 5). The main feature of both measured and predicted data is the very large dip in TL at 170 Hz, the frequency of the lowest transverse wall resonance. This is so pronounced that internally propagated random noise could be heard outside the duct to have a predominantly tonal character. Below this fundamental resonance, the TL *rises* with decreasing frequency, because here the wall impedance is stiffness controlled. A second but less severe wall resonance is evident at 1 kHz. A 3 dB/octave line would not provide a good overall description of the shape of this TL curve in the low-frequency region. Although the construction of this particular duct was perhaps atypical, the behaviour of the TL illustrates the important role that wall resonance effects can play in certain cases, especially where the duct cross-section is square, leading to a relatively high fundamental wall resonance frequency [11].

The discussion in section 2.1 centres on the question of coupled structural/acoustic modes, and if—as in reference [21]—one employs a coupled mode model to find the wall

response, the question arises concerning which modes are to be included in the TL calculation (of course, a treatment that does not include coupling between the internal sound field and the wall vibration also excludes the possibility of "structural"-type modes). Above the lowest transverse wall resonance frequency, there can, in principle, be more than one coupled mode propagating in the duct. We ask, which of these possible modes should be included in our TL model, and what will their amplitudes be? Cummings [21] solved the dispersion equation (2) numerically by the use of Newton's method, but these solutions were invariably of the acoustic type.

In fact, Newton's method will not generally work for finding the structural mode roots of (2), because of the nature of the function on the left side of that equation. None of the commonly used numerical methods appears to be suited to solving this equation for structural modes (this problem is not universal and in FE methods, for example, the structural modes emerge as a part of the process of finding the eigenvalues). Inclusion of the acoustic mode only at a given frequency still gives good predictions of the TL, even though there is the possibility of propagation of structural modes too. Cummings [11] demonstrated that structural-type coupled modes could be exclusively generated by direct excitation of the duct walls, and showed good agreement between predicted and measured axial wavenumbers, but did not cast light on the role of structural-type modes in the TL mechanism. Since structural-type coupled modes generally have a much lower phase speed than acoustic-type modes, they will radiate much less well to the exterior [7, 8]. A partial answer to the first question above is that since the acoustic-type mode (at any given frequency) is likely to dominate the radiated sound field, it is most important that this mode should be included in the formulation. If this mode only is included, we have an essentially "forced-wave" approach. Structural-type modes appear to have a rather passive, minor, role and as long as significant energy is not transferred to them from the acoustic-type mode, their role in TL predictions can be largely ignored. An answer to the second question above will be deferred to section 2.7.

One factor that has not been satisfactorily resolved to date is the question of the structural loss factor to be included in duct wall TL computations, particularly in the case of rectangular ducts. The author has found (e.g., in references [9, 25, 27]) that it is necessary to use an anomalously high structural loss factor—of the order of 0·1—in order that predicted and measured TLs should agree well in the neighbourhood of duct wall resonances. Such a high loss factor is much greater than the internal damping present in the wall material and cannot be explained by "radiation damping", since it is still necessary even when the coupling between wall vibration and the external sound field is taken into account [9].

2.2.2. *Circular and distorted circular cross-sections*

Perfectly circular ducts have a very high wall TL at low frequencies for the plane internal mode, but this falls at about 9 dB/octave and then two dips in the TL curve appear, one near the ring frequency and one near the critical frequency for wave coincidence. Above these frequencies, the TL rises steeply. A predicted TL plot [10] for an ideally circular section air-moving duct of typical construction is shown in Figure 8(a), together with measured data. The measured data were taken on a "long seam" duct, i.e., one with a single, axial, seam; this seam is associated with a significant degree of flattening of the duct wall on either side of it. The predicted plot is based on an "uncoupled" structural/acoustic model. The very high predicted plane mode TL values at low frequencies arise because—for plane-wave excitation—the walls of an ideally circular duct are subjected only to membrane stress, and therefore present a very high impedance to the internal sound wave. It can be seen that the measured TL for this duct at low frequencies falls far below the ideal duct

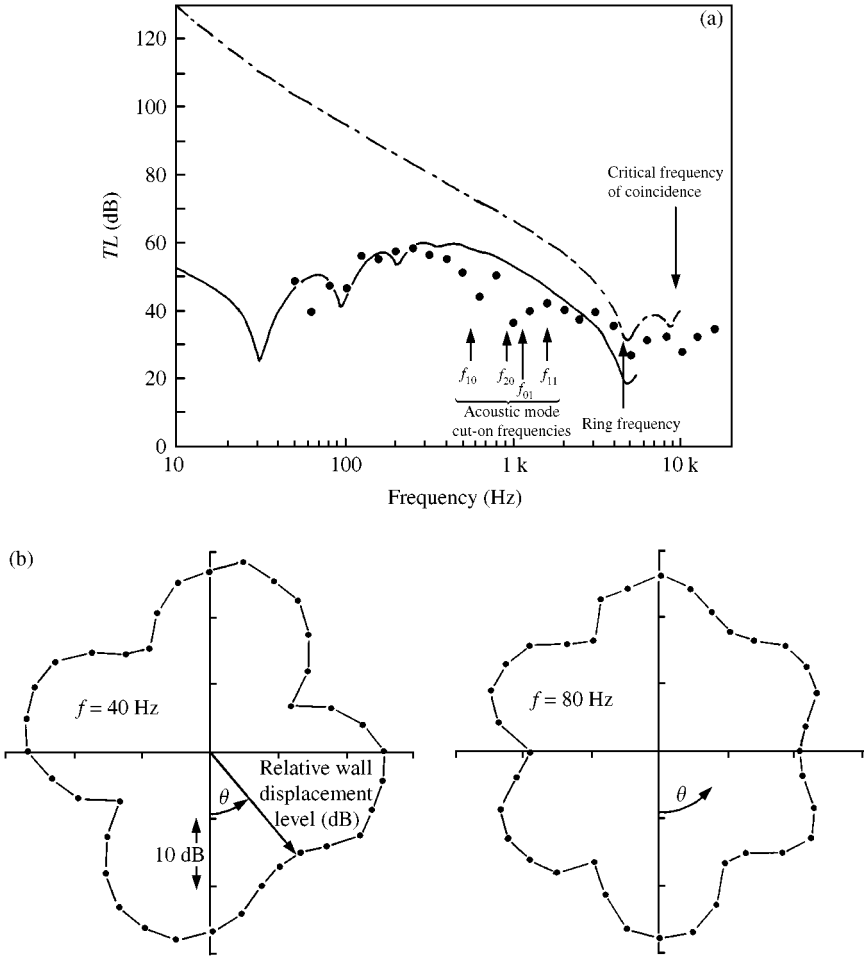

Figure 8. (a) Predicted and measured transmission loss of a "long-seam" circular duct [10] (galvanized steel, diameter 356 mm, wall thickness 1·22 mm). ●, measured data; — – —, TL from ideally circular duct model; ———, TL from distorted circular duct model; (b) Measured circumferential wall vibration patterns on the wall of the long-seam duct at two frequencies [10].

predictions, by as much as 60 dB at 63 Hz. The main reason for this is that the duct is significantly distorted from circularity of cross-section. Heckl [39] noted this, as did Bentley and Firth [40]. Yousri and Fahy [16], Firth [17], Heckl and Ramamurti [18], and Fox [41] all presented theoretical treatments of the structural response of the walls of fluid-filled pipes and cylindrical shells to an internal sound field. Cummings *et al.* [10], and Cummings and Chang [19] modelled both the pipe wall response to an internal sound field and the external structural radiation for distorted circular ducts, leading to TL predictions. For the plane internal acoustic mode, this phenomenon can be termed "mode coupling", since it involves the excitation of *higher* structural modes in the duct wall by non-zero generalized forces arising from the duct wall distortion, and generated by the internal sound field.

A predicted TL plot for the plane internal acoustic mode, taken from reference [10], is also shown in Figure 8(a), where the wall distortion of the duct is taken into account. This is in much better agreement with the measured data, and offers convincing evidence that it is the wall distortion that is responsible for the additional sound radiation, over and

above that emanating from an undistorted duct. It can also be seen that, where higher order acoustic modes can propagate in the duct, the TL falls significantly below the predicted TL for the distorted duct over a two-octave wide band centered on 1 kHz. This is not surprising, since these higher order modes can excite higher structural modes, causing enhanced structural radiation. In Figure 8(b) are shown measured circumferential wall vibration patterns at 40 and 80 Hz, respectively, for the distorted circular duct whose TL is shown in Figure 8(a). These are characteristic of the structural $m = 2$ and 3 circumferential mode patterns of an undistorted shell having otherwise the same parameters, and the frequencies of measurement correspond to those of predicted peak response in these modes, of a distorted circular cylinder excited by the plane acoustic mode. Of course, many other structural modes will be excited at these frequencies, which explains why the displacement amplitude does not more closely approach zero at its minima. But these measured vibration patterns offer further evidence of the role of wall distortion in enhancing the total radiated sound power from the duct wall. In computing the sound power radiated by these higher structure modes, one has to account for their modal radiation efficiencies, and—although these decrease rapidly at low frequencies with increasing mode order—the fact that the higher structural modes are very much more strongly excited that the $m = 0$ breathing mode results in a considerable net increase in radiated sound power.

2.2.3. *Flat–oval cross-section*

Flat–oval ducts have the geometrical features of both rectangular and circular ducts, with two opposite flat walls and two opposite semicircular walls. As mentioned in the introduction, the dynamic behaviour of the wall vibration is actually a hybrid between that of rectangular and circular ducts. At low- to mid-frequencies, the wall TL has a positive slope of about 3 dB/octave, with damped resonances superimposed on it. A ring resonance (for the equivalent circular duct composed of the two semicircular walls joined together) appears at the expected frequency. Measured and predicted TL data on a typical galvanized steel flat–oval duct are shown in Figure 9; these are taken from reference [24]. The predicted TL given by the solid line is derived from a FD solution of the equations of motion for a cylindrical shell of arbitrary geometry and an equivalent cylinder radiation model (see reference [10] and section 2.3). The dashed line is derived from a mass-law impedance model for the flat walls and a circular–cylinder model for the curved walls. These are assumed to contribute independently to the wall displacement. Both predicted TL curves are based on plane mode sound propagation inside the duct and do not include coupling between the internal sound field and the wall motion. The TL is well predicted by both treatments up to 800 Hz, above which frequency both theoretical curves tend to overestimate the TL. This is likely to be caused in part by higher order mode acoustic propagation within the duct. Chang and Cummings [25] report a study of higher order mode effects on the TL of flat–oval ducts, in which this problem in prediction is partially resolved by the inclusion of several higher order modes in the computation. This approach can becomes cumbersome, however, and they suggest a statistical approach as being more appropriate when many modes can propagate. The solid TL line in Figure 9 clearly shows a fundamental resonance at 12 Hz (equivalent to that in a rectangular duct) and a slope of about 3 dB/octave up to 3·5 kHz, with resonant undulations superimposed on it. A pronounced ring resonance is apparent at 6·4 kHz. The measured data also show this ring resonance. Other predicted and measured TL data for flat–oval ducts follow similar patterns to those in Figure 9.

Computed wall displacement patterns (from the FD formulation) at three frequencies on another galvanized steel flat–oval duct are shown in Figure 10. The fundamental wall

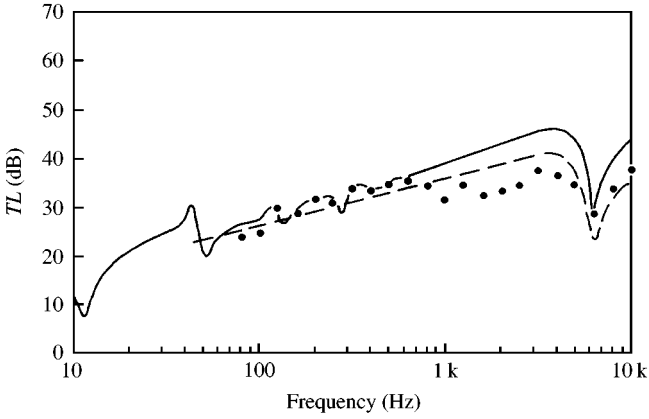

Figure 9. Transmission loss of a 776 mm × 254 mm flat-oval galvanized steel duct with 0·64 mm walls [24]. ●, measured data; ———, FD formulation; — — —, mass law/circular cylinder model.

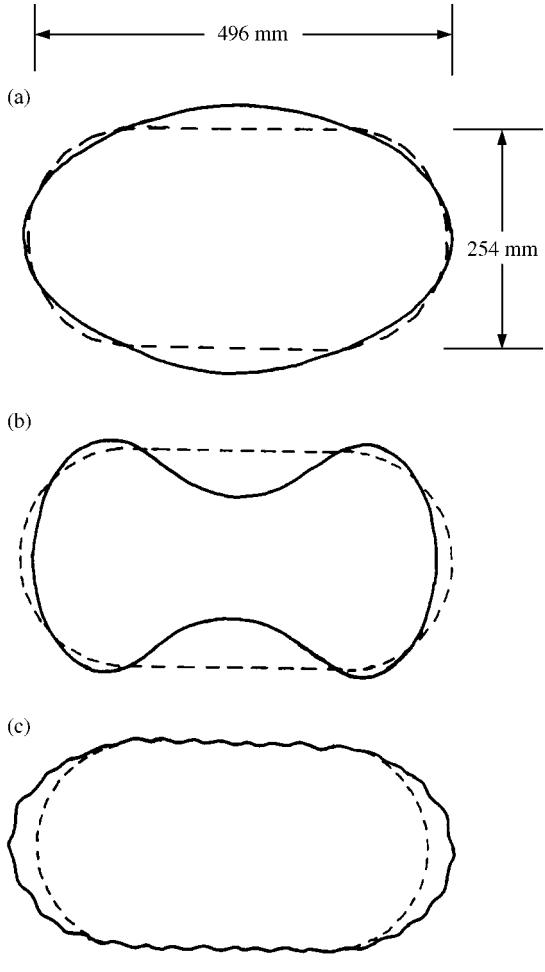

Figure 10. Computed perimetral wall displacement patterns [24], ———, on a flat–oval galvanized steel duct with 0·64 mm walls: (a) 20 Hz, (b) 50 Hz, (c) 6·2 kHz.

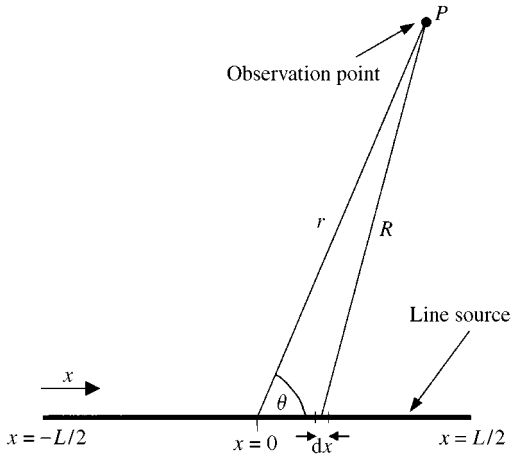

Figure 11. A finite-length line source.

resonance frequency in this case was 35 Hz. The sound pressure within the duct was taken to be at its maximum positive value in all three cases. At 20 Hz, the displacement of the curved walls is very small, while the flat walls are bowed outward. The wall impedance is clearly stiffness controlled, since the displacement and sound pressure are in phase. At 50 Hz, above the fundamental wall resonance, the flat walls display a mass-like impedance, in which displacement and pressure are out of phase. At 6·2 kHz (close to the ring resonance frequency), the motion of the flat walls is limited to a series of short-wavelength undulations, but the curved walls show a significant overall breathing mode behaviour, consistent with the existence of a ring-type resonance. Measured vibration data around the duct perimeter are broadly in agreement with the predictions in Figure 10.

2.3. ACOUSTIC RADIATION FROM THE DUCT WALLS

An integral part of duct wall TL prediction is the calculation of the radiated sound power from the duct walls, based on knowledge of the vibration field of the walls. This requires an appropriate model for the radiation. Perhaps the simplest appropriate radiation model for acoustic radiation from duct walls is the line source formulation of Brown and Rennison [7]. In this, it is assumed that the ratio between a characteristic transverse dimension of the duct and the acoustic wavelength is sufficiently small that the duct walls effectively vibrate like a line monopole distribution of finite length, the source strength per unit length of which is equal to the duct wall displacement, integrated around the duct wall perimeter, at any point. The line source is assumed to be situated in a free field, and the geometry is shown in Figure 11. The volume velocity per unit length is $V(x, t)$, and the sound pressure at the field point P (at position vector $\mathbf{r}$ with respect to the centre of the source), from the source element dx, is

$$p(\mathbf{r}, t) = \rho \, \mathrm{d}x \, \dot{V}(x, t - R/c)/4\pi R, \tag{5}$$

where $R = |\mathbf{r}|$. If one assumes the presence of peristaltic structural waves travelling in both directions [8], i.e.,

$$V(x, t) = [A \exp(-\mathrm{i}k_x x) + B \exp(\mathrm{i}k_x x + \phi)] \exp(\mathrm{i}\omega t), \tag{6}$$

A, B being the wave amplitudes and ϕ a phase angle, then this expression may be inserted into the expression for the farfield mean-squared sound pressure at P,

$$\overline{p^2(\mathbf{r})} = (\rho^2/16\pi^2) \int_{-L/2}^{L/2} \int_{-L/2}^{L/2} \frac{\overline{\mathrm{Re}[\dot{V}(x_1, t - R_1/c)]\,\mathrm{Re}[\dot{V}(x_2, t - R_2/c)]}}{R_1 R_2}\,\mathrm{d}x_1\,\mathrm{d}x_2, \quad (7)$$

where $R_1 \approx r - x_1 \cos\theta$, $R_2 \approx r - x_2 \cos\theta$. The resultant expression for sound intensity is then integrated over a spherical surface to yield the radiated sound power,

$$W = (\rho\omega L/8\pi)[(A^2 + B^2)\,[1/\chi_1 - 1/\chi_2 - \cos\chi_1/\chi_1 + \cos\chi_2/\chi_2 - \mathrm{Si}(\chi_1) + \mathrm{Si}(\chi_2)] + (2AB\cos\phi/K)\{\cos K\,[\mathrm{Cin}(\chi_1) - \mathrm{Cin}(\chi_2)] - \sin K\,[\mathrm{Si}(\chi_1) - \mathrm{Si}(\chi_2)]\}, \quad (8)$$

where $K = k_x L$, $\chi_1 = K - kL$, $\chi_2 = K + kL$ and Si( ), Cin( ) are the sine integral and the modified cosine integral respectively [42]. A "radiation efficiency" may be defined as

$$C_r = W/[\rho\omega(A^2 + B^2)/8], \quad (9)$$

where the expression on the denominator is the sound power that would be radiated from the source if it were infinitely long and $k_x < k$ (supersonic wave speed). Brown and Rennison [7] considered the situation where $B = 0$ and $\chi_2 \gg 1$, and plotted C_r against χ_1. For $\chi_1 = 0$ (i.e., a sonic wave speed), $C_r = 0{\cdot}5$. This figure is a reasonable approximation to the radiation efficiency for ducts away from wall resonance frequencies (so that the wave speed is approximately sonic) and for the duct length greater than about an acoustic wavelength.

This simple model is adequate for radiation from ducts in which the internal sound field is dominated by the plane mode, even at frequencies where the acoustic wavelength is of the order of the larger duct dimension. But it is inadequate where one considers higher order mode propagation within the duct. Take, for example, the lowest cross-mode propagating in a rectangular duct. Clearly, since the internal sound pressure distribution is antisymmetric, the wall displacement profile will be too, and so $V(x, t) = 0$ under all conditions, because of volume velocity cancellation around the wall perimeter. Therefore, no sound at all would radiate from the duct walls according to the above model, and this is clearly incorrect. An advance on the simple line source model is the "cylindrical radiator" model of Cummings [27]. In this, an "equivalent" infinitely long cylindrical radiator of radius R is considered, with the same perimeter as the actual duct (whatever its cross-sectional shape), and having the actual perimetral surface velocity distribution *produced by a single internal acoustic mode* extended around its perimeter. It is relatively straightforward to calculate the sound power radiated from such a duct. This result may be written

$$W_\infty = \frac{\omega\rho}{k_r^2}\left[\frac{|a_0|^2}{2|Q_0|^2} + \sum_{j=1}^{\infty} \frac{|a_j|^2 + |b_j|^2}{|Q_j|^2}\right], \quad (10)$$

where $k_r = \sqrt{k^2 - k_x^2}$, a_j and b_j are the Fourier coefficients of the wall velocity amplitude around the duct perimeter and $Q_j = (1/k_r)(\partial/\partial r)H_j^{(2)}(k_r r)|_{r=R}$. An heuristic approach (doubtless no worse than the above approximation) is then taken in writing an expression for the radiated sound power from the duct as

$$W = W_\infty C_r, \quad (11)$$

where C_r is found from the line source model above. The actual distribution of surface velocity on the duct wall is accounted for, and so are the finite length of the source and the structural wave speed. In reference [27], coupling between the internal sound field and the wall vibration was neglected and so k_x is simply the acoustic modal axial wavenumber. The shape of the radiating body is not properly taken into account, but this turns out to make little difference to the accuracy of numerical predictions. Astley and Cummings [9] reported FE computations of the TL of rectangular ducts for higher order mode internal sound propagation. The duct wall response was found by means of an FE solution scheme in which the wall vibration was taken to be uncoupled to the internal sound field but coupled to the radiated sound field. (Internal acoustic/structural coupling could straightforwardly have been taken into account, but it was not considered necessary to do so in this study.) An external FE solution region was matched to a cylindrical radiating surface and W_∞ determined, i.e., for an infinitely long duct. W was then found by the use of equation (11). This method represents a further improvement on that of Cummings [27] in that the geometry of the radiating surface is correctly modelled. Comparisons [9] between the FE model and the cylindrical radiator model showed generally very close correspondence between the radiated sound power computed from the two models, even for ducts of high cross-sectional aspect ratio (the maximum differences being only about 2–3 dB, with discrepancies in most cases being much smaller than this).

A more accurate representation of sound radiation from a finite length radiating section on an otherwise rigid infinite cylinder is given by Cummings *et al.* [10], and based on the analysis of Junger and Feit [43]. This involves writing an outgoing wave solution of the Fourier-transformed Helmholtz equation, matching this to the surface vibration pattern on the cylinder (assumed to correspond to a travelling wave in one direction only) and carrying out the inverse transform by the use of the method of stationary phase to yield the farfield sound pressure. If the circumferential vibrational displacement pattern is expressed as a cosine Fourier series with coefficients ξ_m, the resulting radiated sound power is

$$W = \frac{4\rho c\omega^2}{\pi} \sum_{m=0}^{\infty} \frac{\xi_m^2}{\varepsilon_m} \int_0^{\pi} \frac{\sin^2 [(k\cos\phi - k_x)L/2]}{\sin\phi |H_m^{(2)'}(kR\sin\phi)|^2 (k\cos\phi - k_x)^2} \, \mathrm{d}\phi, \tag{12}$$

ε_m being a Neumann symbol and R, L the radius and length of the radiating section of cylinder. This integration is readily performed numerically, and the summation is truncated at an appropriate point. The contributions from the terms in the summation in this expression are, in effect, from multipole line radiators of increasingly high order as m increases. As expected, their radiation efficiencies (defined in an appropriate way) fall dramatically at low frequencies as m increases, though this dependence on order is less pronounced at higher frequencies, as is the case with other types of multipole radiator. The effects of the rigid end extensions on the cylinder are not obvious from equation (12), and Cummings *et al.* [10] also carried out FE computations of sound radiation from a cylinder of *finite length*—with rigid "end caps" but without the end extensions—for comparison purposes. They concluded that the end extensions made a negligible difference to the radiated sound field, for practical purposes.

2.4. RECIPROCITY RELATIONSHIPS FOR BREAKOUT AND BREAKIN

So far, acoustic breakout through duct walls has been discussed with little reference to breakin. But sound transmission into ducts from an external sound field can be of equal importance, particularly where flanking mechanisms of various kinds are concerned, e.g.,

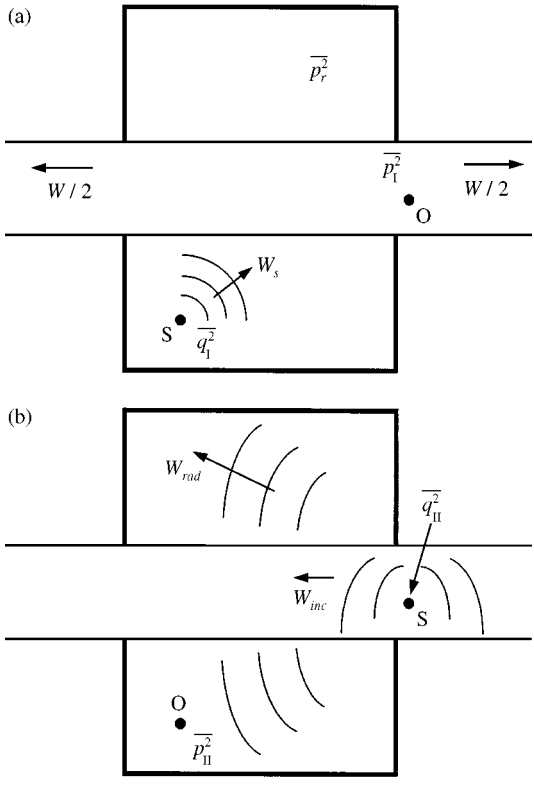

Figure 12. Reciprocity in breakout/breakin: (a) source in room; (b) source in duct.

"cross-talk" between internal building spaces caused by breakin and subsequent breakout in ventilation ducts [15], and "radiation bypass" flanking in duct silencers [3]. The modelling of sound transmission into a duct from a reverberant sound field appears to be a formidable task to accomplish directly, and the author knows of no publications in which attempts to do this have been reported. However, simple relationships between the breakout and breakin TLs of duct walls may readily be derived by the use of reciprocity relationships. The familiar principle of reciprocity in acoustics is also valid where flexible boundaries such as plates are present, as Lyamshev [44] has shown. Vér [45] has made use of the reciprocity principle in work related to acoustic breakout and breakin in ducts. The principle is used here without proof or experimental validation, though proofs are readily available in reference [44] and elsewhere.

A relationship between the breakout TL of duct walls, as defined in equation (3)—which may be termed TL_{out}—and the breakin TL, correspondingly denoted TL_{in}, may be derived as follows. Consider a duct (of semi-infinite extent in both directions, and assumed to carry only the fundamental acoustic mode) passing through a room, as shown in Figure 12. First of all, let there be a point harmonic monopole source S (mean-squared volume velocity $\overline{q_I^2}$) in the room and an "observer" O (e.g., a microphone), at which the mean-squared sound pressure is $\overline{p_I^2}$, in the duct, as shown in Figure 12(a). Next, consider the reciprocal situation with the source and observer interchanged, as shown in Figure 12(b); here the mean-squared

volume velocity of the source and the observed mean-squared sound pressure are $\overline{q_{\text{II}}^2}$ and $\overline{p_{\text{II}}^2}$ respectively. The reciprocity theorem tells us that

$$\overline{p_{\text{I}}^2}/\overline{q_{\text{I}}^2} = \overline{p_{\text{II}}^2}/\overline{q_{\text{II}}^2}. \tag{13}$$

The sound power directly radiated by the source into the room for the case in Figure 12(a) may be taken to be the freefield value,

$$W_s = \rho\omega^2\,\overline{q_{\text{I}}^2}/4\pi c \tag{14}$$

and the resulting reverberant field mean-squared sound pressure (neglecting the direct field contribution) may be expressed by elementary geometrical acoustics as

$$\overline{p_r^2} = 4\,\rho c W_s/R = \rho\omega^2\,\overline{q_{\text{I}}^2}/\pi R, \tag{15}$$

where R is the room constant. If we consider W to be the total breakin sound power (split equally into two equal power flows of $W/2$ between the two duct sections) resulting from the incident reverberant sound field, then the duct-borne power flow to the right in Figure 12(a) may be related to $\overline{p_{\text{I}}^2}$ by expression

$$W/2 = \overline{p_{\text{I}}^2} A/\rho c_x, \tag{16}$$

where A is the cross-sectional area of the duct and c_x is the phase speed of the fundamental mode in the duct. Equations (14–16) may be combined to yield

$$\overline{p_{\text{I}}^2}/\overline{q_{\text{I}}^2} = (W/2)\rho^3 c_x \omega^2/A\overline{p_r^2}\,\pi R. \tag{17}$$

For the case in Figure 12(b), the sound power radiated into the duct by the point source is

$$W_{inc} = \overline{q_{\text{II}}^2}\,\rho\omega^2/4A|k_x|^2 c_x, \tag{18}$$

which covers the case where k_x is complex (i.e., there is axial attenuation in the duct). We also have the reverberant field contribution to the mean-squared sound pressure in the room,

$$\overline{p_{\text{II}}^2} = 4\rho c W_{rad} R \tag{19}$$

and from the definition of TL_{out} (equation (3)). we may say

$$W_{inc} = W_{rad}(A/PL)10^{TL_{out}/10}. \tag{20}$$

Equations (18–20) may be combined to yield

$$\overline{p_{\text{II}}^2}/\overline{q_{\text{II}}^2} = \rho^2\omega^2 cPL10^{-TL_{out}}/RA^2|k_x|^2 c_x. \tag{21}$$

Now, equations (15, 17, 21) may be combined to yield

$$W/2 = W_s 4\pi c^2 PL10^{-TL_{out}}/RAc_x^2|k_x|^2, \tag{22}$$

which relates the transmitted breakin sound power in each half of the duct to the sound power radiated by the point source. We may choose to define

$$TL_{in} = 10\log[(\overline{p_r^2}/4\rho c)/(W/2A)], \tag{23}$$

i.e., the logarithmic ratio between the sound power per unit area incident from the reverberant field on the exterior surface of the duct to the total internally transmitted sound power per unit area. A relationship between TL_{in} and TL_{out} is then found from equations (15, 22, 23),

$$TL_{in} = TL_{out} + 10\log(A^2 c_x^2 |k_x|^2 / 4\pi c^2 PL). \tag{24}$$

If the imaginary part of k_x is small (i.e., the axial attenuation rate is small) and $c_x \approx c$, equation (24) becomes

$$TL_{in} = TL_{out} + 10\log(A^2 k^2 / 4\pi PL). \tag{25}$$

Other possible definitions of TL_{in} exist, of course, but it is clear that the breakout and breakin transmission losses may be related by simple formulae similar to those above, subject to some reasonable approximations.

2.5. NATURAL DUCT ATTENUATION, INTERNAL LINING AND FLANKING MECHANISMS

In this section, breakout/breakin effects are discussed in the contexts of both unlined ducts—in which case they give rise to natural duct attenuation—and lined ducts, in which case they are associated with radiation bypass flanking, together with direct structural flanking.

2.5.1. *Natural duct attenuation*

So-called natural duct attenuation is usually taken into account by HVAC engineers in noise control calculations that involve air-moving ducts. Until relatively recently, when Cummings [4] presented an analysis of this effect for rectangular section ducts, the attenuation mechanisms do not appear to have been quantified, though it had been generally realized (see e.g., reference [46]) that "energy losses because of duct wall vibration" were responsible. Attenuation in unlined ducts is of most significance in the case of rectangular section ducts, and so the discussion here will be restricted to this case. A flexible-walled duct passing through a reverberant space (room constant R) is shown in Figure 13; it will be assumed that only the fundamental internal acoustic mode propagates. In the *absence* of breakin, sound power W_1 is incident in the duct from the left side of the room. Of this, W_0 is radiated—via breakout—into the room, W_d is dissipated by damping in the walls and the remainder, W_2, is transmitted in the duct to the right. A sound power balance equation may be written

$$W_1 = W_0 + W_d + W_2. \tag{26}$$

But in reality breakin will also occur, manifesting itself as a power flow W_i, which splits equally between the two halves of the duct. An *average* attenuation rate (including the effects of breakin), in dB per unit distance along the duct, may be defined

$$\Delta = (10/L)\log[W_1/(W_2 + W_i/20)], \tag{27}$$

where L is the duct length. Once appropriate expressions for W_d, W_i, etc., have been found (W_i being determined on the basis of the reciprocity relationships described in section 2.4),

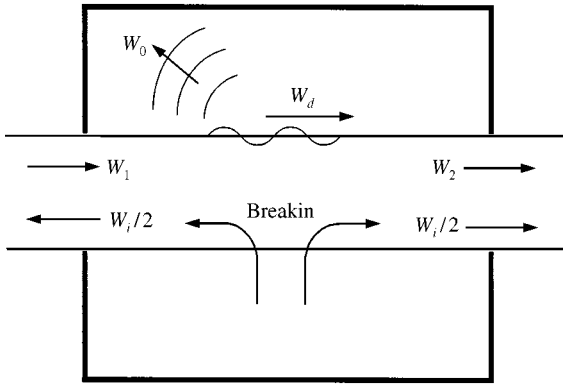

Figure 13. Power flow in an unlined duct passing through a reverberant enclosure.

an expression for Δ may be written [4]

$$\Delta = (10/L)\log\{1/(1-(PL/A)[|1-P_e/P_i|^2(c_x/c)\,\mathrm{Re}\,\langle\beta\rangle\,[1-\exp(2L\,\mathrm{Im}\,(k_x))]/(-2L\,\mathrm{Im}\,(k_x))$$
$$+\,10^{-TL/10}\{1-(PL/A)10^{-TL/10}(4\pi c^2/c_x^2)/R|k_x|^2\}])\}, \tag{28}$$

where P_i and P_e are the sound pressure amplitudes inside the duct and on its outer surface (the latter being found on the basis of a cylindrical radiator model), TL is the breakout transmission loss and the other symbols are as defined previously (β being defined in terms of the sound pressure *differential* across the duct walls). The terms in the denominator in the outer set of curly brackets may be identified as follows. The first term in the outer set of square brackets represents wall dissipation losses and the first and second terms in the inner curly brackets, represent breakout and breakin sound power respectively. If R tends to infinity (corresponding to freefield conditions) for instance, the breakin sound power term vanishes, as one would expect. If TL becomes very large, then both breakout and breakin terms become negligibly small. Equation (28) is deceptively simple, and a fairly complicated iterative scheme is actually required to find $k_x, \langle\beta\rangle, TL$ and hence Δ. The reason for this is that k_x is defined as being complex, consistent with sound power radiation by the duct walls. This can only be found once TL is known, but TL depends on $\langle\beta\rangle$, which in turn depends on k_x. For the sake of tractability, it is assumed that acoustic radiation from the duct walls is uniform along the length of the duct, though in reality this would not be the case. A comparison between numerical predictions [4] and measured data from a report by Nelson and Burnett [47] (the only publication which, to the author's knowledge, contains the necessary information about the reverberant enclosure surrounding the duct) is shown in Figure 14. The peaks in the predicted plot of Δ occur around duct wall resonance frequencies, and can be as high as 4 dB/m (at 50 Hz). This is a very useful degree of attenuation, particularly at such a low frequency, where dissipative attenuators would perform very poorly. Quantitative agreement between prediction and measurement is surprisingly good up to 800 Hz, especially since the tests reported in reference [47] were not specifically intended for the measurement of unlined duct attenuation, but rather the breakout and breakin TLs. Furthermore, sound pressure level—rather than sound power—was recorded by Nelson and Burnett and W_1 was inferred here from the *total* sound pressure level (including the contribution from $W_i/2$) in the tests. This was not though to have incurred a significant error, however. The peaks in the predicted attenuation are fairly

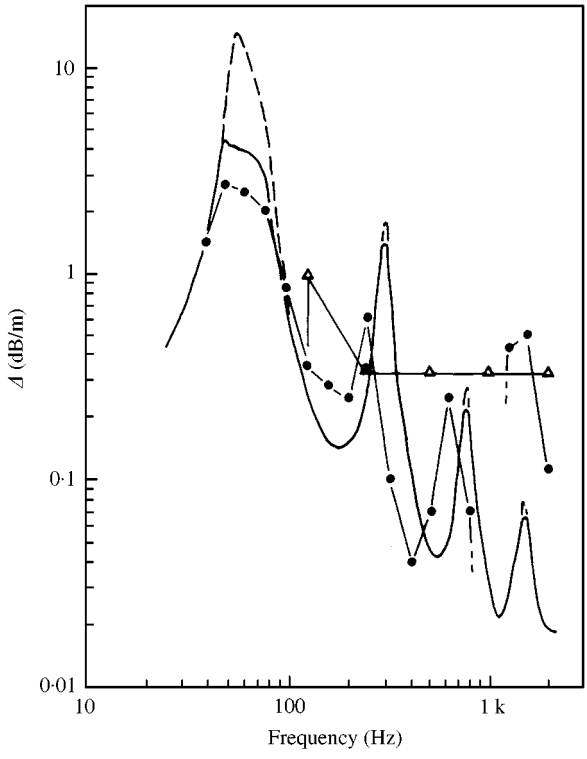

Figure 14. Predicted and measured attenuation rate in a 300 mm square galvanized steel duct with 0·91 mm walls. ●——●, measured data [47]; ———, predicted with breakin [4]; — — —, predicted without breakin [4]; △——△, ASHRAE prediction [46].

close to those in the measured data, and the attenuation figures agree tolerably well. A predicted plot without breakin is also shown, and it can be seen that this overestimates the peak attenuation by about a factor of 4. The predictions from the ASHRAE method [46] are plotted too, and can be seen to give quite poor predictions of the natural duct attenuation.

Duct wall breakout (and, to a lesser extent, breakin) clearly dominates Δ and, as one would expect, the peaks in attenuation all occur around the wall resonance frequencies. Clearly, a simplistic prediction method such as the ASHRAE scheme [46], which does not allow for all the relevant physical effects, cannot hope to yield satisfactory predictions and a more complete predictive method must be employed.

2.5.2. *Internal lining and flanking*

Reference has been made in section 2.1 to some of the effects that the combination of a sound-absorbing duct lining and flexible walls can have. Astley [38], Cummings *et al.* [48], Astley *et al.* [13], and Kirby and Cummings [30, 31] have all examined coupled mode solutions in acoustically lined ducts with flexible walls. The results behave in a generally similar way, and in Figure 15 are shown FE axial attenuation rate predictions by Kirby and Cummings [30] for the first three coupled modes in a small square-section lined duct. For zero gas flow ($M = 0$, where M is the mean flow Mach number—assumed uniform—in the central open flow passage) mode I exhibits a very substantial peak at about 220 Hz as

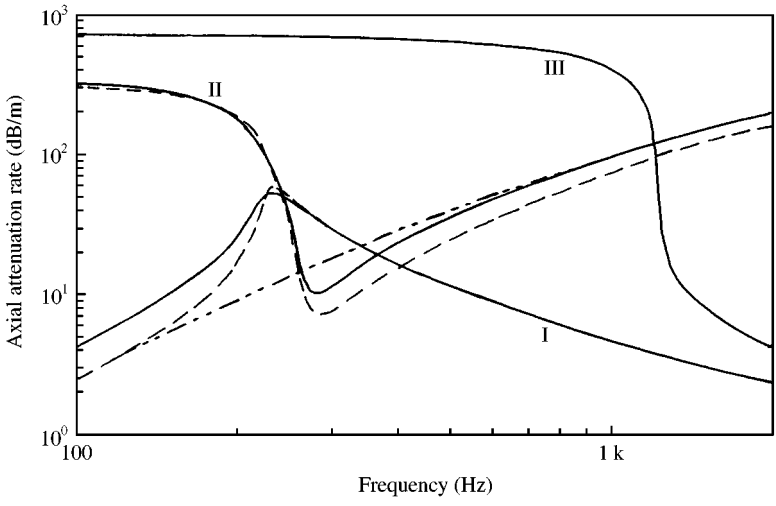

Figure 15. FE predicted axial attenuation rate of coupled modes in an acoustically lined duct 107 mm square, with 0·54 mm galvanized steel walls, having a 26·8 mm glass fibre internal lining on all four walls [30]. ———, $M = 0$; — — —, $M = 0{\cdot}1$; — – – —, least attenuated mode in lined rigid-walled duct, $M = 0$.

compared to the rigid-wall case. This phenomenon has been explained in section 2.1. Mode II is highly attenuated at low frequencies but its attenuation falls very sharply around the peak in mode I, and above this frequency it follows the rigid-wall curve fairly closely. Mode III is even more highly attenuated at low frequencies, but its attenuation falls rapidly at about 1.2 kHz. The behaviour of the real part of the axial wavenumber in lined ducts broadly resembles that in unlined ducts (see section 2.1), though the "cut-on" phenomena for the higher modes differ in detail.

Cummings and Astley [14] specifically examined lined ducts with a view to establishing the nature of both radiation bypass and direct structural flanking mechanisms in a relatively simple system consisting of an internally lined duct, anechiocally terminated and with a sound source at the opposite end, situated in a reverberant chamber. The method of analysis of coupled modes involved the application of the Rayleigh–Ritz procedure, involving a simple three-degree-of-freedom trial function for the internal sound pressure distribution and a three-d.o.f. trial function for the wall displacement. The principle of reciprocity was used to include the breakin sound pressure from the reverberant sound field outside the duct. This is valid, not only in the presence of flexible boundaries, but also where layers of bulk-reacting absorbent exist. A series of coupled structural/acoustic modes was matched to the sound source (structural as well as acoustic boundary conditions having to be satisfied in this process). In this way, the excitation of "structural"-type modes, that turn out to be relatively lightly damped and are capable of giving rise to direct structural flanking, was taken into account. The total mean-squared acoustic pressure inside the duct, along the axis, was expressed as the sum of the mean-squared pressure *without* breakin and the mean-squared pressure component *arising from* breakin. This problem encapsulates the essential physical phenomena that govern attenuation and both types of flanking mechanism, and gives a general indication of the effects to be anticipated in much more complex systems such as package silencers. It should be noted, however, that in systems incorporating axial discontinuities, acoustic-type coupled modes could be partially transformed into structural-type coupled modes and *vice versa*. This effect is absent in the simpler case discussed here. The behaviour of such discontinuities is discussed in section 2.7.

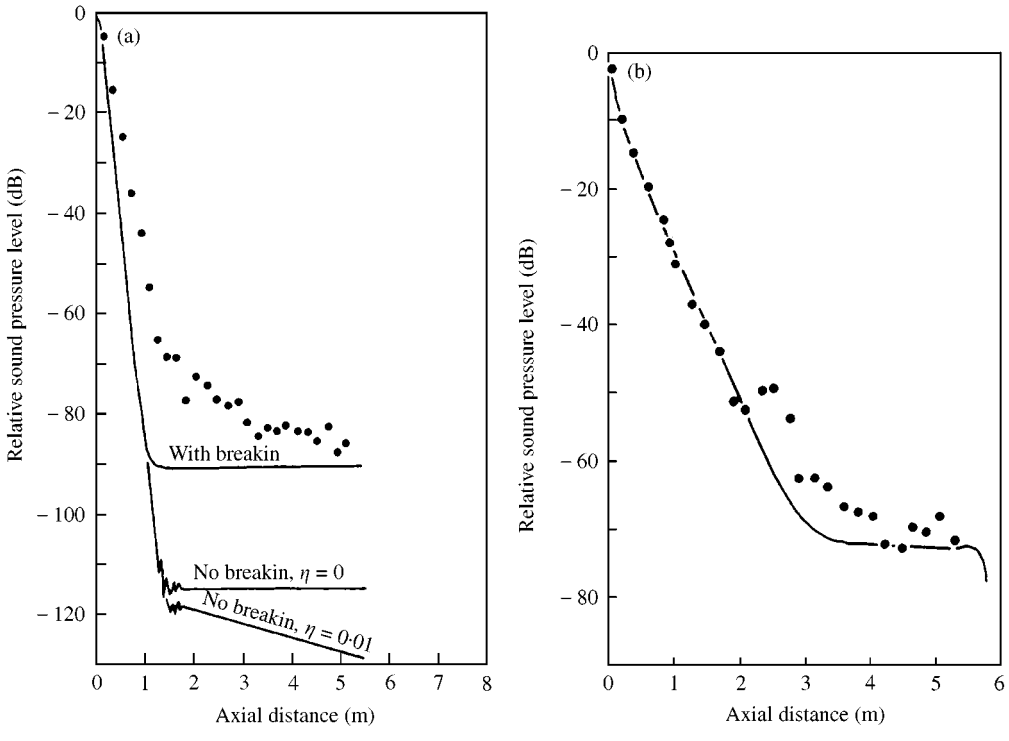

Figure 16. Predicted and measured sound pressure level at (a) 1·6 kHz, (b) 500 Hz along the axis of an acoustically lined galvanized steel duct (300 mm square section, 0·58 mm walls, with 53 mm semi-rigid glass fibre lining on all four walls), placed in a reverberant room [14]. ●, measured L_p; ———, predicted L_p with breakin (or without breakin in (a)).

In Figure 16(a, b) are shown the predicted and measured axial sound pressure levels (L_p) as a function of axial distance from the sound source, from reference [14], at 1·6 kHz and 500 Hz. The test duct was 300 mm square in section, was fabricated from 0·58 mm galvanized steel and was lined with 53 mm semi-rigid glass fibre slab on all four walls. In Figure 16(a), predictions are plotted both with and without breakin. There are two plots without breakin, for two values of the structural loss factor η. It is seen that the measured L_p falls rapidly with increasing distance from the source, but then levels out at about -85 dB, relative to the level at the source. The predicted plot with breakin shows a similar pattern, with a plateau at -90 dB. Without breakin—after the initial sharp fall in L_p and a series of undulations—a plateau at -115 dB is evident in the predicted plot with $\eta = 0$, while the curve for $\eta = 0{\cdot}1$ initially has the same shape, but instead of having a plateau, it falls gently with distance from the source. The second parts of the curves without breakin represent direct structural flanking caused by lightly damped structural-type coupled modes. The acoustic-type coupled mode which dominates the sound field up to a distance about 1·5 m from the source is heavily damped and ceases to make a significant contribution to the total mean-squared sound pressure beyond that distance. With $\eta = 0$, the axial variation in L_p is so small as to be imperceptible, while for $\eta = 0{\cdot}1$, structural damping lends this same mode some degree of axial attenuation. The separate role of structural-type coupled modes is quite clear in this example: they closely resemble free structural waves, and there is so little acoustic motion associated with them that vibrational energy flow can bypass the acoustic lining in the duct with negligible attenuation. By contrast, the predicted curve with radiation bypass flanking (i.e., breakout/breakin) is in

quantitatively fair and qualitatively good agreement with the measured data. The discrepancies between prediction and measurement are probably attributable largely to inadequacies in the trial functions employed in the Rayleigh–Ritz formulation. In this particular case, one may see that radiation bypass flanking dominates the effects of direct structural flanking, though whether this is more generally true requires further investigation. Another comparison between prediction and measurement at 500 Hz for this case is shown in Figure 16(b). Quite good agreement between prediction and measurement is evident here; at this lower frequency, the trial functions give a better representation of the vibro-acoustic field in the duct.

The results shown in Figure 16 are qualitatively similar to data discussed by Vér [49], who plotted the measured sound insertion loss of a 25 mm internal sound-absorbing duct lining in a 660 mm square sheet metal duct against length of lining for various frequencies. He found that a levelling-off of the insertion loss occurred beyond a certain length of liner, most markedly at 1·25 kHz, less so at 400 Hz and not at all 125 Hz. This was attributed by Vér to "flanking through bending waves travelling in the duct wall", though the mechanism was not investigated further. Without a knowledge of all relevant details of Vér's experiments, one cannot accurately identify the dominant flanking mechanism, but it seems likely that radiation bypass may have been the main contributor.

2.6. THE EFFECTS OF MEAN GAS FLOW

In Figure 15, plots of axial attenuation rate are shown for $M = 0$ and 0·1 (the mean flow is in the direction of sound propagation). Mean flow can be seen to lower the axial attenuation rate of mode I up to the fundamental duct wall resonance frequency at 220 Hz, where the mode is predominantly "acoustic" in character. This lowering of attenuation at relatively low frequencies is well known in rigid-walled ducts with acoustic linings (see e.g., reference [50]); at higher frequencies, the reverse effect tends to occur. Above 220 Hz there is little flow effect on attenuation since the energy flow is now mainly in the structure. This is not surprising, since the structural motion is only weakly coupled to the vibrational field of the duct wall for structural-type coupled modes and would not be strongly affected by the convective and refractive effects of mean flow in the lined central portion of the duct. Mean flow also affects the imaginary part of the axial wavenumber (not shown here), and for mode I, the axial phase speed is increased as one would expect. When mode I undergoes a transition to a structural-type mode, the effect of flow on the phase speed disappears, for the reason stated above. To an extent, therefore, mean gas flow serves to discriminate between predominantly acoustic and predominantly structural types of coupled wave motion.

More generally, moderate mean flow—at speeds typical in air-moving ducts—does not have a dramatic effect on breakout and breakin. In unlined ducts [51], its main effect is to alter the axial wavenumber in the duct, which in turn has a small effect on the wall vibration amplitude in the coupled structural/acoustic modes and on the radiation efficiency, but the effects on the duct wall TL are, in the main, likely to be small.

2.7. AXIAL DISCONTINUITIES

Although—as we have seen—very successful TL predictions may be made on the basis of the acoustic type coupled mode only, for lengths of duct largely uninterrupted by structural or acoustic discontinuities, it is important to know what the effects of various types of axial discontinuity might be in other cases. Such discontinuities may be in the form of flanges or

other kinds of joint between sections of duct, cross-sectional area changes or silencer terminations. It is possible that energy could be transferred from the acoustic-type mode to one or more structural-type modes at an axial discontinuity, and that these could act as direct structural flanking paths, perhaps across a silencer. In general terms, it is clearly necessary, in systems that embody discontinuities, to know the distribution of energy flow between the various coupled modes.

The experimental duct system studied by Astley *et al.* [13] embodied a source loudspeaker radiating into a rigid-walled, acoustically lined, rectangular duct, one wall of which underwent a transition to a flexible wall. This wall was rigidly clamped along both edges, and was also rigidly clamped to the rigid duct section. An FE analysis was employed to solve the structural/acoustic eigenvalue problem so as to yield a series of coupled travelling modes in the flexible-walled duct. This series of coupled modes was then matched to the rigid-wall acoustic modes in the duct section between the flexible section and the sound source. Point collocation was used to match the acoustic pressure and axial particle velocity on the duct cross-section in the plane containing the structural discontinuity (this was straightforward, since the FE mesh was identical in both regions), and the structural boundary conditions of zero wall displacement and zero slope were also satisfied in the flexible wall in this plane. It was assumed that only the least attenuated acoustic mode was incident on the discontinuity from the source, and the coefficients of the reflected acoustic modes in the rigid duct section and the transmitted coupled modes were found from the mode-matching process. (The duct was terminated anechoically both for acoustic and structural waves.) The computed and measured axial displacement amplitude pattern on the centreline of the flexible wall at 300 Hz are compared in Figure 17; the computed pattern is found as a summation of coupled modes. Predictions and measurements compare quite well. The pattern resembles a standing wave with an axially decaying maximum amplitude, but is composed principally of the lowest two coupled modes, both propagating in the *same* direction with different axial phase speeds. The *difference between* these speeds gives rise to the observed phase interference pattern. The two dominant coupled modes are excited such that their structural amplitudes at the discontinuity are roughly equal and they are in almost opposite phase at this point. This would be expected, since the two modes must approximately cancel in order to satisfy the structural boundary condition of zero displacement, assuming the contributions from other modes are small. (The zero slope boundary condition would require a certain higher order mode content for its satisfaction.) The measured axial sound pressure pattern within the duct (not shown here) has undulations superimposed on a steady fall in level along the flexible-walled section, but these are much less pronounced than in the case of the wall vibration because of the relatively small sound pressure in the second, structural type, mode as compared to the first, acoustic type, mode.

The nature of the structural displacement pattern shown in Figure 17 is very characteristic of those observed in the same problem of a rigid/flexible transition in a duct *without* an acoustical lining. In this case, however, there is very little fall-off in maximum vibration amplitude. Where more than one coupled mode can propagate, this type of pattern always prevails, though it can become more complex at high frequencies, where modes with a very non-uniform sound pressure pattern (the equivalent of higher acoustic modes in a rigid-walled duct) can propagate. One can anticipate a similar behaviour in actual air-moving ducts, where higher, structural-type, coupled modes (behaving essentially like free structural waves) coexist with the acoustic-type mode. These structural-type modes would radiate poorly, play a minor role in the sound radiation process (see the discussion in section 2.2.1), and exist—in a sense—in order to satisfy the structural boundary conditions at discontinuities such as flanges. Martin [29] observed structural "standing wave" patterns

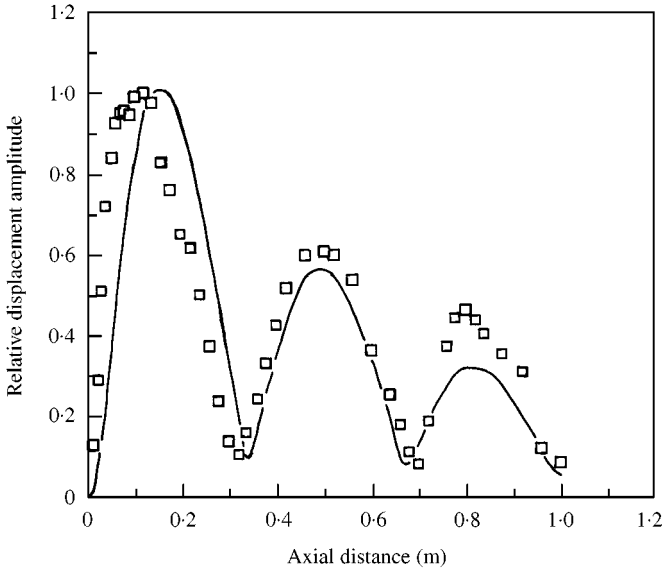

Figure 17. Computed and measured axial distribution of the vibration displacement amplitude on the centreline of the flexible wall of a lined duct having three rigid walls and one flexible wall [13] (transverse duct dimensions 90 mm × 100 mm; one of the 100 mm walls is of 0·54 mm aluminium plate). □, measured data; ———, FE computed data.

in his (wooden) experimental duct, which are likely to be caused, at least in part, by the above mechanism. However, Martin's duct embodied transverse reinforcing members at regular intervals, and these no doubt played a part in generating higher coupled modes.

Cummings and Astley [14] prove that the coupled modes in a duct with a bulk-reacting linear and no mean flow are orthogonal on a region consisting of the duct interior (including the lining) and the duct walls. This orthogonality relationship obviously also applies to unlined ducts. In reference [14], a weighted residual mode-matching procedure is employed to find the coefficients of the coupled modes. The modal orthogonality relationship is used in this process and yields a straightforward algebraic relationship for the modal coefficients.

The "second question" in section 2.2.1, concerning the relative amplitudes of coupled modes, is answered in general terms by the foregoing discussion.

3. THE REDUCTION OF BREAKOUT AND BREAKIN NOISE

In this section, methods that may be used to reduce breakout and breakin effects in ducts are discussed. These are of two types, first involving the design of ducts for high TL over the frequency range of interest, and secondly the application of noise reduction treatment to existing ducts, where noise problems are found to exist.

3.1. STIFFENING THE DUCT WALLS

As mentioned in the Introduction, one way of increasing the breakout TL of rectangular ducts is to increase the ratio between the flexural rigidity and the mass/unit area of the walls

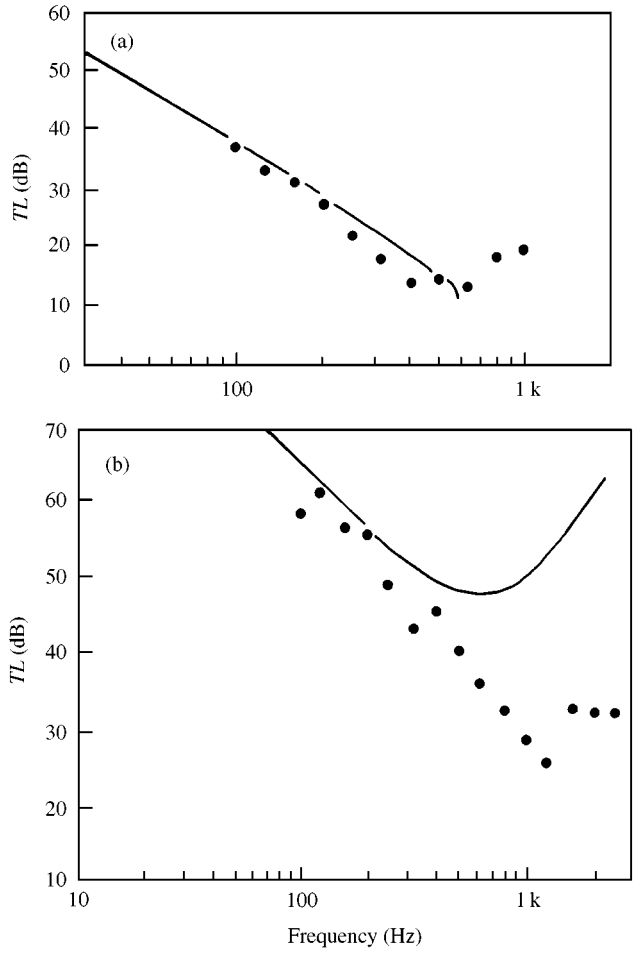

Figure 18. Transmission loss of stiff-walled square section ducts [11]. ●, measured data. (a) Expanded polystyrene duct walls: ———, theoretical curve for rigid duct corners. (b) Composite sandwich duct walls: ———, theoretical curve for pin-jointed duct corners.

[11]. This raises the fundamental transverse structural resonance frequency of the walls and essentially shifts the low-frequency portion of the TL curve—where the TL increases with falling frequency—to higher frequencies, thereby providing benefits in the crucial low-frequency region where the levels of noise propagating in the duct are usually highest. This approach is not likely to be applicable to ducts of very large transverse dimensions and would best be used in the case of ducts with square, rather than rectangular, cross-section since the fundamental wall resonance will occur at a considerably higher frequency for a square duct than for a rectangular duct of similar dimensions [11].

Two examples of this method, applied to ducts of fairly small square cross-section and taken from reference [11], are shown in Figure 18. Predicted and measured TL data on an expanded polystyrene duct of 241 mm square cross-section (measured to the central plane of opposite walls) and 38 mm thick walls are shown in Figure 18(a). Although the mass/unit area of the duct walls was only 0·67 kg/m^2, the very high stiffness/mass ratio of the duct walls caused the fundamental transverse wall resonance to occur at 480 Hz. At 100 Hz, the

wall TL is 37 dB, and it falls to about 13–14 dB in the region of 400–600 Hz before rising again. Prediction and measurement agree fairly well up to about 600 Hz. This duct is not very practical in view of its poor fire resistance, but it does demonstrate the principle of stiffening the walls. In Figure 18(b) are shown measured TL data for a duct of 216 mm square cross-section with walls consisting of two 0·91 mm aluminium sheets with a resinated paper honeycomb core bonded to them. The overall wall thickness was about 13 mm. The predicted TL for a duct with pin-jointed corners is shown (the duct walls were so stiff that the corner fixing corresponded more closely to a pin joint than a rigid corner). Correspondence between prediction and measurement is reasonable up to 200 Hz but less good above this frequency. At all events, the TL does attain very high values, being about 61 dB at 125 Hz. The minimum TL is about 25 dB. A quasi-steady low-frequency TL approximation is given in reference [11],

$$TL = 10\log\{E^2h^6(a+b)/36(1-v^2)^2\rho^2c\omega^3[(a^3+b^3)^2/72(a+b) + ab(a^2-b^2)(a-b)/48 - (a^5+b^5)/80]^2\}, \tag{29}$$

where a, b are the transverse duct dimensions, E and v are Young's modulus and the Poisson's ratio of the duct wall material and h is the wall thickness. Criteria for the accuracy of the approximation to within 1 dB are as follows. If we define $g = Eh^3/12(1-v^2)$ and $\gamma = \omega^{1/2}(m/g)^{1/4}$, the criteria are that (1) $\gamma a < 3$ for a square section duct, (2) γa, $\gamma b < 2$ for a non-square duct, (3) $\gamma a > 2ka$ for either case. All these criteria represent upper limiting frequencies.

Circular ducts have inherently superior TL characteristics to those of rectangular ducts at low frequencies as previously discussed, and another possibility for noise control at the design stage would be to select a circular-section duct in preference to a rectangular duct. If space considerations (e.g., in a "ceiling void") precluded this choice, a flat–oval duct would still be superior in its TL characteristics to a rectangular duct.

3.2. THE APPLICATION OF EXTERNAL LAGGING

External lagging is an "add-on" treatment that is sometimes used as a curative measure in the case of ducts that have been found to cause noise problems. It usually consists of a layer of fibrous material such as glass fibre blanket, covered with a layer of massive material such as plaster, sheet metal or a plastic material. It would not normally be necessary to apply lagging to circular ducts, and it is likely that it is employed most commonly to rectangular ducts. Cummings [34] reports a method of modelling external lagging on rectangular ducts, partially involving the use of electrical analogues, in which the external lagging is modelled as a rectangular tube with elastic walls. A comparison is shown in Figure 19 between prediction and measurement of the acoustic insertion loss (IL) of external lagging consisting of a 25 mm thick rockwool blanket, covered with a 0·38 mm thick tinned steel sheet. This was applied to a duct 203 mm square, with 1·22 mm thick steel walls. Agreement between prediction and measurement is fairly good. The upper frequency limit in the computed plot was imposed by ill-conditioning of the matrix involved in solving the equations of motion for the lagging, brought about by the low flexural rigidity of the external lagging covering. The main point of interest, however, is that at 125 and 250 Hz, the lagging actually *exacerbates* the problem to a significant degree. As more degrees of freedom are introduced into the system, the possibility of untoward resonance effects is increased, and in this case resonances at these two frequencies between the duct wall and the lagging covering cause the lagging to have a negative insertion loss.

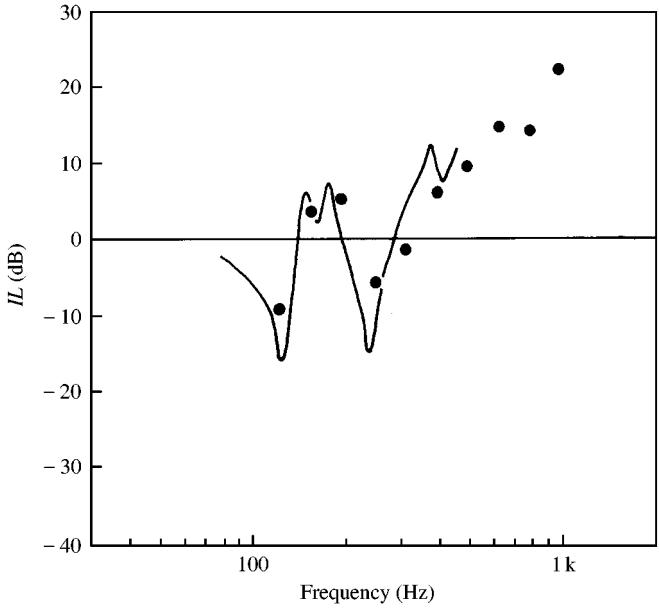

Figure 19. Measured and predicted insertion loss of tinned steel/rockwool external lagging applied to a 203 mm square section mild steel duct with 1·22 mm walls [34]. ●, measured IL; ———, predicted IL (analytical method).

Another set of measured data, from reference [52], is shown in Figure 20. In this case, a 60 mm glass fibre blanket was applied to a 762 mm × 457 mm flat–oval duct, and covered with a layer of vinyl sheet with $m = 2{\cdot}84$ kg/m^2. An IL prediction, from a semi-empirical method [52], is also shown in Figure 20. Although an IL in excess of 30 dB was obtained from this lagging design, it still has an IL of about -3 dB at 125 Hz. More generally, the IL of typical external lagging would normally be small—often of the order of 0–5 dB—in the important low-frequency region below about 200 Hz, and in some cases the IL can actually be negative. One can conclude that, if external lagging is to be used in an attempt to cure a duct breakout noise problem, care should be exercised in its design so as to avoid low-frequency resonance effects.

4. DISCUSSION

During the past two decades, considerable progress has been made in the quantitative understanding of noise transmission through the walls of ducts, both in the identification of the physical mechanisms governing the sound transmission process and in the prediction of breakout and breakin TLs, etc. The author has played his part in this, along with many other researchers. Various methods of analysis—from analytical solutions to numerical formulations—have been applied to the problem of breakout. The propagation of sound in ducts with elastic walls, the structural excitation of the walls, the radiation to the exterior and the nature of the structural/acoustic coupling, are all important features of the sound transmission process and significant progress has been made in the modelling of these phenomena.

But is also clear that much remains to be done. For example, the relative roles of the structural and acoustic types of coupled modes in sound transmission remain to be further

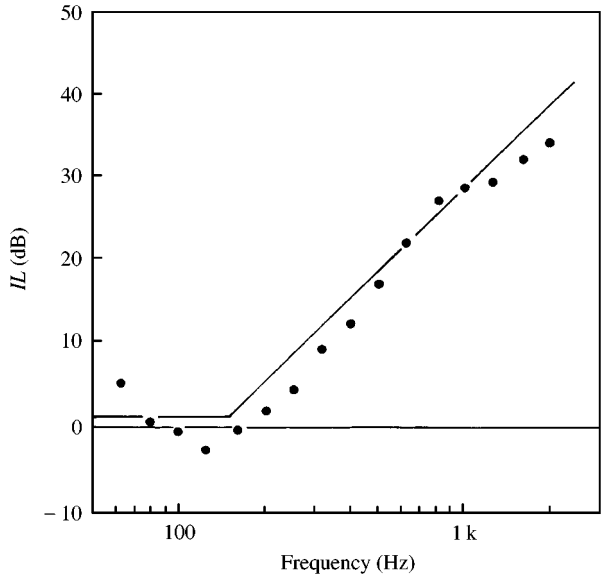

Figure 20. Measured and predicted insertion loss of vinyl sheet/glass fibre blanket external lagging, applied to a 762 mm × 457 mm flat–oval galvanized steel duct with 0·64 mm walls [52]. ●, measured *IL*; ———, predicted *IL* (semi-empirical method).

clarified. Ways of modelling complex systems such as commercial package silencers, in which—for example—a variety of flanking paths exists, need to be developed. An obvious possibility for such complex systems would be to consider the usefulness of SEA methods, which are particularly well suited to the analysis of sound and vibration transmission in systems with multiple components. It would probably be necessary to develop new subsystem models, especially those in which significant energy dissipation occurs. A disadvantage of SEA is that it does not work well at low frequencies, where modal densities are low. This is, however, exactly the frequency region where it is most important to have accurate predictive modelling methods available, and this might suggest that an SEA approach would be inappropriate. Purely numerical techniques such as FE methods are probably the best means of yielding accurate predictions of whatever performance parameters are required to describe the system. Assuming all relevant material properties and boundary conditions are known to the required degree of accuracy, and the system has been correctly modelled, there is no obvious reason why such methods could not yield valuable engineering design data. With the current rate of development of computing power it seems likely that the complexity of the system to be analyzed might not necessarily preclude the application of numerical methods in the case of HVAC applications, though the same could not be said of other, much more complex, systems such as entire aircraft. However, the effort required in creating numerical models of relatively complex HVAC systems would be considerable, and it is unlikely that they would gain popular acceptance as engineering design tools.

What other possibilities exist for the development of predictive methods that can be applied to realistic HVAC duct systems? Analytical techniques can only be applied to fairly simple systems, and cannot generally cope with the complexities of practical types of duct and silencer, although they are always invaluable as a benchmark against which (say) numerical predictions can be compared. It has been shown here that some of these methods can yield quite accurate predictions if the actual system is somewhat idealized, but it

could not be claimed that this philosophy would be likely to form a sound basis for robust design methods. The author believes that it might be possible to develop a general framework—perhaps as an extension of existing transfer matrix formulations and involving multiple branched energy flow paths—in which relatively simple "subsystem" elements can be modelled and linked together in an ordered manner, enabling highly complex systems to be analysed. Such a "building block" approach could, perhaps, also be applied to other types of vibro-acoustic systems in much the same manner as SEA, though with completely different physical principles as its basis.

ACKNOWLEDGMENT

Some of the work referred to here (in references [30, 31, 51]) was carried out with financial support from the European Commission, under Brite-EuRam project no. BRPR CT97-0394.

REFERENCES

1. J. D. WEBB 1972 *Noise Control in Mechanical Services*. Colchester: Sound Attenuators Ltd., Sound Research Laboratories Ltd. See chapter 9.
2. I. SHARLAND 1972 *Woods Practical Guide to Noise Control*. Colchester: Woods Acoustics. See chapter 5.
3. F. P. MECHEL 1975 *Transactions of Inter-Noise* **75**, Sendai, Japan, 751–760. Design criteria for industrial mufflers.
4. A. CUMMINGS 1994 *Journal of Sound and Vibration* **174**, 433–450. The attenuation of sound in unlined ducts with flexible walls.
5. M. K. BULL and M. P. NORTON 1980 *Journal of Sound and Vibration* **69**, 1–11. The proximity of coincidence and acoustic cut-off frequencies in relation to acoustic radiation from pipes with disturbed internal turbulent flow.
6. A. CUMMINGS 1983 *Journal of Sound and Vibration* **90**, 211–227. Approximate asymptotic solutions for acoustic transmission through the walls of rectangular ducts.
7. G. L. BROWN and D. C. RENNISON 1974 *Proceedings of the Noise, Shock and Vibration Conference, Monash University, Melbourne*, 416–425. Sound radiation from pipes excited by plane acoustic waves.
8. A. CUMMINGS 1980 *Journal of Sound and Vibration* **71**, 201–226. Low frequency acoustic radiation from duct walls.
9. R. J. ASTLEY and A. CUMMINGS 1984 *Journal of Sound and Vibration* **92**, 387–409. A finite element scheme for acoustic transmission through the walls of rectangular ducts: comparison with experiment.
10. A. CUMMINGS, I.-J. CHANG and R. J. ASTLEY 1984 *Journal of Sound and Vibration* **97**, 261–286. Sound transmission at low frequencies through the walls of distorted circular ducts.
11. A. CUMMINGS 1981 *Journal of Sound and Vibration* **74**, 351–380. Stiffness control of low frequency acoustic transmission through the walls of rectangular ducts.
12. A. CABELLI 1985 *Journal of Sound and Vibration* **103**, 379–394. The propagation of sound in a square duct with a non-rigid side wall.
13. R. J. ASTLEY, A. CUMMINGS and N. SORMAZ 1991 *Journal of Sound and Vibration* **150**, 119–138. A finite element scheme for acoustical propagation in flexible walled ducts with bulk reacting liners, and comparison with experiment.
14. A. CUMMINGS and R. J. ASTLEY 1995 *Journal of Sound and Vibration* **179**, 617–646. The effects of flanking transmission on sound attenuation in lined ducts.
15. C. H. ALLEN 1960 in *Noise Reduction* (L. L. Beranek, editor). New York: McGraw-Hill. See chapter 21.
16. S. N. YOURSI and F. J. FAHY 1977 *Journal of Sound and Vibration* **52**, 441–452. Distorted cylindrical shell response to internal acoustic excitation below the cut-off frequency.
17. D. FIRTH 1978 *International Journal for Numerical Methods in Engineering* **13**, 151–164. Acoustic vibration of a liquid filled distorted circular cylindrical shell.

18. M. HECKL and V. RAMAMURTI 1979 *Acustica* **43**, 313–318. Schalldämmung von Rohren mit elliptischen Querschnitt.
19. A. CUMMINGS and I.-J. CHANG 1986 *Journal of Sound and Vibration* **104**, 377–393. A finite difference scheme for acoustic transmission through the walls of distorted circular ducts and comparison with experiment.
20. G. F. KUHN and C. L. MORFEY 1976 *Journal of Sound and Vibration* **47**, 147–161. Transmission of low-frequency internal sound through pipe walls.
21. A. CUMMINGS 1978 *Journal of Sound and Vibration* **61**, 327–345. Low frequency acoustic transmission through the walls of rectangular ducts.
22. A. CUMMINGS 1979 *Journal of Sound and Vibration* **63**, 463–465. Low frequency sound transmission through the walls of rectangular ducts: further comments.
23. A. GUTHRIE 1979 *M.Sc. Dissertation, Polytechnic of the South Bank*. Low frequency acoustic transmission through the walls of various types of ducts.
24. A. CUMMINGS and I.-J. CHANG 1986 *Journal of Sound and Vibration* **106**, 17–33. Noise breakout from flat-oval ducts.
25. I.-J. CHANG and A. CUMMINGS 1986 *Journal of Sound and Vibration* **108**, 157–164. Higher order mode and multimode acoustic transmission through the walls of flat–oval ducts.
26. A. CUMMINGS and I.-J. CHANG 1986 *Journal of Sound and Vibration* **106**, 35–43. Sound propagation in a flat–oval waveguide.
27. A. CUMMINGS 1983 *Journal of Sound and Vibration* **90**, 193–209. Higher order mode acoustic transmission through the walls of rectangular ducts.
28. A. CABELLI 1985 *Journal of Sound and Vibration* **103**, 13–23. Application of the time dependent finite difference theory to the study of sound and vibration interactions in ducts.
29. V. MARTIN 1991 *Journal of Sound and Vibration* **144**, 331–353. Perturbation of fluid-guided waves introduced by bending plates.
30. R. KIRBY and A. CUMMINGS 1998 *Proceedings of ISMA*23, *Leuven, Belgium*, 677–684. Structural/acoustic interaction in air-conditioning ducts in the presence of mean flow.
31. R. KIRBY and A. CUMMINGS *Paper presented at the Forum Acusticum/ASA Conference, Berlin, Germany*, 14–19 *March* 1999. The effects of flanking transmission on sound attenuation in lined air-conditioning ducts.
32. A. CUMMINGS 1981 *Journal of Sound and Vibration* **78**, 269–289. Design charts for low frequency acoustic transmission through the walls of rectangular ducts.
33. ASHRAE 1984 *ASHRAE Handbook*—1984 *Systems*. Atlanta, GA: American Society of Heating, Refrigerating, and Air-Conditioning Engineering. See chapter 32.
34. A. CUMMINGS 1979 *Journal of Sound and Vibration* **67**, 187–201. The effects of external lagging on low frequency sound transmission through the walls of rectangular ducts.
35. A. CUMMINGS 1983 *University of Missouri-Rolla Department of Mechanical and Aerospace Engineering Final Contract Report on ASHRAE RP*-318. Acoustic noise transmission through the walls of air-conditioning ducts.
36. M. ALMGREN 1982 *Chalmers University of Technology Department of Building Acoustics Report F*82-03. Prediction of sound pressure level outside a closed ventilation duct—a literature survey.
37. F. J. FAHY 1985 *Sound and Structural Vibration*. London: Academic Press. See chapter 6.
38. R. J. ASTLEY 1990 *Proceedings of Inter-Noise* 90, Gothenburg, Sweden, 575–578. Acoustical modes in lined ducts with flexible walls: a variational approach.
39. M. HECKL 1958 *Acustica* **8**, 259–265. Experimentelle Untersuchungen zur Schalldämmung von Zylindern.
40. P. G. BENTLEY and D. FIRTH 1971 *Journal of Sound and Vibration* **19**, 179–191. Acoustically excited vibrations in a liquid-filled tank.
41. M. J. H. FOX 1979 *Central Electricity Generating Board Report RD/B/N*4617. The response of distorted pipes to internal acoustic excitation.
42. M. ABRAMOWITZ and I. A. STEGUN 1965 *Handbook of Mathematical Functions*. New York: Dover Publications.
43. M. C. JUNGER and D. FEIT 1972 *Sound, Structures and Their Interaction*. Cambridge, MA: MIT Press. See sections 8.10–8.12.
44. L. M. LYAMSHEV *Soviet Physics—Doklady* **4**, 406–409. A question in connection with the principle of reciprocity in acoustics.
45. I. L. VÉR 1983 *American Society of Heating, Refrigerating and Air-Conditioning Engineers Final Contract Report TRP*-319. Prediction of sound transmission through duct walls; breakout and pickup.

46. ASHRAE 1987 *HVAC Handbook*. Atlanta, GA: American Society of Heating, Refrigerating and Air-Conditioning Engineers. See pp. 52.9–52.10.
47. P. A. NELSON and R. BURNETT 1981 *Technical Report No. TRC* 107, *Sound Attenuators Ltd*. Laboratory measurements of breakout and break-in of sound through walls of rectangular ducts.
48. A. CUMMINGS, R. J. ASTLEY and N. SORMAZ 1990 *Proceedings of the Institute of Acoustics* **12**, 865–872. The influence of wall flexibility on sound propagation in a duct with bulk-reacting liners.
49. I. L. VÉR 1978 *American Society of Heating, Refrigerating and Air-Conditioning Engineers Transactions* **84**, 122–149. A review of the attenuation of sound in straight lined and unlined ductwork of rectangular cross-section.
50. A. CUMMINGS 1976 *Journal of Sound and Vibration* **49**, 9–35. Sound attenuation in ducts lined on two opposite walls with porous materials, with some applications to splitters.
51. R. KIRBY and A. CUMMINGS 1998 *EC Brite/Euram Project no. BRPR CT*97-0394 1st *Annual Report*. Modelling sound generation and propagation in fluid machinery systems. See Annex C.
52. A. CUMMINGS 1985 *American Society of Heating, Refrigerating and Air-Conditioning Engineers Transactions* **91**, 48–61. Acoustic noise transmission through ducts walls.